Enhanced functional expression of the polyhydroxyalkanoate synthase gene from *Cupriavidus necator* A-04 using a cold-shock promoter for efficient poly(3-hydroxybutyrate) production in *Escherichia coli*

Thanawat Boontip
Chulalongkorn University Faculty of Science
Rungaroon Waditee-Sirisattha
Chulalongkorn University Faculty of Science
Kohsuke Honda
Osaka university
Suchada Chanprateep NAPATHORN (suchada.cha@chula.ac.th)
Chulalongkorn University Faculty of Science https://orcid.org/0000-0002-3598-9344

Research

Keywords: poly(3-hydroxybutyrate), pCold, chaperone, trigger factor, Cupriavidus necator

Posted Date: September 22nd, 2020

DOI: https://doi.org/10.21203/rs.3.rs-28241/v2

Version of Record: A version of this preprint was published at Frontiers in Bioengineering and Biotechnology on June 3rd, 2021. See the published version at https://doi.org/10.3389/fbioe.2021.666036.

Abstract

Background: The present study attempted to increase polyhydroxybutyrate (PHB) production by improving the functional expression of the *PhaC* gene using various types of promoters, and the effects on PhaC activity in terms of PHB productivity, yield coefficient ($Y_{P/S}$) and molecular weights were investigated.

Results: Here, the PHB biosynthesis operon of *Cupriavidus necator* A-04, isolated in Thailand with a high degree of 16S rRNA sequence similarity with *C. necator* H16, was subcloned into pGEX-6P-1, pColdI, pColdTF, pBAD/Thio-TOPO and pUC19 (native promoter) and transformed into *E. coli* JM109. To alter the expression of *phaCAB* biosynthesis genes, we optimized parameters in flask experiments to obtain high expression of soluble $PhaC_{A-04}$ protein with high $Y_{P/S}$ and PHB productivity. pColdTF-*phaCAB*$_{A-04}$-expressing *E. coli* produced 2.5±0.1 g/L (90.6±4.3%) PHB in 24 h, similar to pColdI-*phaCAB*$_{A-04}$-expressing *E. coli*. The amounts of phaC protein and PHB produced from pColdTF-*phaCAB*$_{A-04}$ and pColdI-*phaCAB*$_{A-04}$ were significantly higher than those from other promoters. Cultivation in a 5-L fermenter led to PHB production of 7.9±0.7 g/L with 90.0±2.3% PHB content in the cell dry mass (CDM), a $Y_{P/S}$ value of 0.38 g PHB/g glucose and a productivity of 0.43 g PHB/(L×h) using pColdTF-*phaCAB*$_{A-04}$. The PHB from pColdTF-*phaCAB*$_{A-04}$ had M_w 5.79×10^5 Da, M_n 1.86×10^5 Da and PDI 3.11 and the film exhibited high transparency, Young's modulus and tensile strength, possibly due to the trigger factor (TF) chaperones. Interestingly, when pColdI-*phaCAB*$_{A-04}$-expressing *E. coli* was used to produce PHB from crude glycerol and compared with pUC19-nativeP-*phaCAB*$_{A-04}$-expressing *E. coli*, the amounts of PHB were similar, but M_w 1.1×10^6 Da, M_n 2.6×10^5 Da and PDI 4.1 were obtained from pUC19-nativeP-*phaCAB*$_{A-04}$-expressing *E. coli,* indicating that slow and low expression could prolong and maintain phaC polymerization activity.

Conclusions: This is the first report to demonstrate that the cspA promoter in a cold-inducible vector can improve $PhaC_{A-04}$ expression levels, and TF chaperones show obvious effects on enhancing $PhaC_{A-04}$ solubility. The high level of $PhaC_{A-04}$ resulted in a high PHB amount, but the chain termination reaction of PhaC polymerization occurred faster than that with the slowed and low expression of $phaC_{A-04}$ by the native promoter pUC19, which resulted in a low amount of high-molecular-weight PHB produced from crude glycerol.

Background

The global environmental concern regarding microplastics in the marine environment as contaminants with significant impacts on animal and human health has led to a call for national and international policies from more than 60 countries to ban or place a levy on single-use plastics [1-4]. Renowned global companies have also integrated regulations and policies to ban single-use plastics into their green marketing and corporate social responsibility policies. Bioplastics are becoming a popular alternative to single-use plastics to reduce the amount of microplastic waste. Recently, the annual production of bioplastics was approximately only one percent of the total 360 million tons of plastics. However, as the market for bioplastics is growing and the demand for bioplastics is rising, European Bioplastics reported that the global bioplastic production capacity will increase from 2.11 million tons in 2019 to approximately 2.43 million tons in 2024 [5]. Among the various types of bioplastics, polyhydroxyalkanoates (PHAs) are an important biodegradable polymer family, as they are one hundred percent biobased and fully biodegradable in all environments, especially marine (ASTM 7081) and fresh water environments [6, 7].

To obtain both the environmental and economic benefits of PHAs over synthetic plastics and other bioplastics, microorganisms that exhibit efficient PHA production from inexpensive and renewable carbon sources are urgently required to develop a low-cost approach. Microbial cells typically accumulate poly(3-hydroxybutyrate) (PHB), the first PHA discovered since 1927 by Maurice Lemoignei of Institut Pasteur in France [8], at approximately 30–50% of the cell dry mass (CDM). The best known industrial PHA producer, *Cupriavidus necator* H16 (formerly known as *Alcaligenes eutrophus*, *Ralstonia eutropha* and *Wautersia eutropha*), is capable of accumulating PHB at over 80% of the CDM. PHA accumulation is tightly regulated by imbalanced growth conditions with excess carbon but limited nitrogen [9]. One of the major limitations in the production of PHAs in wild-type strains has been intracellular polymer degradation caused by endogenous PHA depolymerases, which is different from the behavior of exogenous PHA depolymerases [10]. Therefore, intracellular PHAs are often spontaneously degraded during cultivation when the bacteria require carbon, resulting in low PHA content and a wide range of molecular weight distributions in wild-type strains. Thus, many recombinant strains have been developed by metabolic engineering to obtain a high yield of PHB and a molecular weight that is high enough for polymer processing [11-16]. Ordinarily, the PHB biosynthesis pathway begins with acetyl-CoA and requires 3 major enzymes, namely, 3-ketothiolase (*phaA*), NADPH-dependent acetoacetyl-CoA reductase (*phaB*), and PHA synthase (*phaC*), and these 3 genes are sufficient for the production of PHB in non-PHA-producing bacteria at more than 90% of the CDM when heterologously expressed in *Escherichia coli* [17]. It has been reported that PhaC plays a key role in obtaining the polymeric form, resulting in a high level and high molecular weight of PHB [14, 16].

To date, PHA synthases have been categorized into four major classes based on their sequence, substrate specificity, and subunit composition [18, 19]. Class I and Class II PHA synthases consist of the PhaC subunit, which is believed to be a homodimer. On the other hand, Class III and IV PHA synthases are heteroclusters comprised of PhaC-PhaE subunits and PhaC-PhaR subunits, respectively. In addition, Class I, III, and IV PHA synthases preferentially polymerize short-chain-length (SCL) monomers comprised of C3-C5 carbon chain lengths, whereas Class II PHA synthases specifically polymerize medium-chain-length (MCL) monomers in the C6-C14 chain length range. It was reported that PhaC derived from *C. necator* H16 ($PhaC_{H16}$) is a Class I PhaC and is one of the most widely studied PHA synthases. It has a molecular weight of approximately 64 kDa (589 amino acids) and is located as the first gene in the PHA biosynthetic phaCAB operon, followed by PhaA and PhaB [20, 21]. It was demonstrated that the weight-average molecular weight (M_W) of PHB synthesized by wild-type bacteria is generally in the range of $0.1–2.0\times10^6$ Da. Because *Escherichia coli* does not contain endogenous PHA

depolymerases, ultrahigh-molecular-weight PHB, which has a defined M_w more than 3.0×10^6 Da and is much larger than the PHB produced by the wild-type strain, can be obtained and used for the development of high-strength fibers and films [22]. The crystal structures of the catalytic domain at 1.48Å resolution acquired by X-ray crystallography for $PhaC_{H16}$ [23, 24] and $PhaC_{Cs}$ from *Chromobacterium* sp. USM2 have already been reported [25]. When recombinant $PhaC_{H16}$ was overexpressed in *E. coli*, most of the protein formed insoluble inclusion bodies due to its low aqueous solubility [26-29]. To feasibly achieve industrial-scale production, PhaC would need to be produced in large quantities and its solubility would need to be improved [30]. There have been many reports that have attempted to resolve the problem mentioned above, including by modulating the concentration of the PhaC protein by varying the chemical inducer quantities [31]; expressing the protein at a reduced temperature (30°C) [30]; fusing the PhaC protein with a glutathione S-transferase (GST) tag, which is a hydrophilic tag, to improve its solubility [32]; and coexpressing the protein with chaperones to obtain high total quantities of enzyme and a larger proportion in the soluble fraction than obtained without chaperones. However, coexpression of the GroEL/GroES chaperone system with the PHA production operon resulted in the production of polymers with reduced molecular weights [30]. In this study, we reported the use of pCold (cspA promoter) to improve PhaC expression as well as its combination with trigger factor (TF) chaperone that have never been reported.

In a previous study, we reported the generation of the *C. necator* strain A-04, possessing 99.78% 16S RNA sequence similarity with *C. necator* H16 but differing in PHA production ability [33]. Designed using the gene walk technique, the PHA biosynthesis operon of *C. necator* strain A-04 consisted of three genes, encoding acetyl-CoA acetyltransferase ($phaA_{A-04}$, 1182 bp, 40.6 kDa, accession no. FJ897461), acetoacetyl-CoA reductase ($phaB_{A-04}$, 741 bp, 26.4 kDa, accession no. FJ897462) and PHB synthase ($phaC_{A-04}$, 1770 bp, 64.3 kDa, accession no. FJ897463). Sequence analysis of the $phaA_{A-04}$, $phaB_{A-04}$ and $phaC_{A-04}$ genes revealed that $phaC_{A-04}$ was 99% similar to $phaC_{H16}$ from *C. necator* H16. The difference was in the amino acid residue situated at position 122, which in $phaC_{A-04}$ was proline but in *C. necator* H16 was leucine. The total amino acid sequences of $phaA_{A-04}$ and $phaB_{A-04}$ were 100% matched with those of *C. necator* H16 [34]. Notably, *C. necator* strain A-04 prefers fructose over glucose as a carbon source, accumulating PHB at 78% of the CDM under a C/N ratio of 200, whereas it could incorporate a high mole fraction of monomeric 4-hydroxybutyrate monomeric into the poly(3-hydroxybutyrate-*co*-4-hydroxybutyrate) [P(3HB-*co*-4HB)] copolymer under a C/N ratio of 20 [35], as well as the poly(3-hydroxybutyrate-*co*-3-hydroxyvaterate-*co*-4-hydroxybutyrate) [P(3HB-*co*-3HV-*co*-4HB)] terpolymer [36]. In this study, to realize the capability of the PHA biosynthesis operon of *C. necator* strain A-04 when heterologously expressed in recombinant *E. coli*, it was amplified via PCR; cloned into pGEX-6P-1 (tac promoter, isopropyl-β-D-thiogalactopyranoside (IPTG)-inducible vector, N-terminal GST fusion protein), pColdI (cspA promoter, cold- and IPTG-inducible vector, N-terminal 6His-fusion protein), pColdTF (cspA promoter, cold- and IPTG-inducible vector, trigger factor (TF) chaperone, N-terminal 6His-fusion protein), pBAD/Thio-TOPO (araBAD promoter, arabinose-inducible vector, N-terminal thioredoxin fusion protein and C-terminal 6His-fusion protein) and pUC19 (control strain, $phaCAB_{A-04}$ biosynthesis genes with native promoter of $phaC_{A-04}$); and transformed into *E. coli* JM109 (Table 1). Next, to optimize $phaC_{A-04}$ overexpression in shake flask cultivation, we tested and compared three induction methods (Figure 1, details are described in the materials and methods section). In this study, we examined the effect of $phaC_{A-04}$ overexpression on PHB production in recombinant *E. coli* with respect to cell growth, glucose consumption, PHB production, and kinetic parameters in conditions ranging from flask culture to a 5-L fermenter. $PhaC_{A-04}$ was purified, quantified, carefully compared versus pColdI-$phaCAB_{A-04}$ and pColdTF-$phaCAB_{A-04}$, and also between short induction and conventional induction methods. Furthermore, the produced PHB was subjected to molecular weight determination, thermal analysis and mechanical property measurement.

Results

Effect of the growth phase on the production of $PhaC_{A-04}$ and PHB by the conventional induction method

To optimize the conditions for heterologous expression of $phaCAB_{A-04}$ biosynthesis genes, after the pColdI-$phaCAB_{A-04}$ and pColdTF-$phaCAB_{A-04}$ vectors were transformed into *E. coli* JM109, expression was induced with 0.5 mM IPTG (final concentration) at different growth phases by varying OD_{600} based on cultivation time: 0.5 (2 h, early exponential phase), 1.3 (4 h, middle exponential phase), 2.1 (6 h, late exponential phase) and 2.4 (10 h, stationary phase). Concurrently, the temperature was shifted from 37°C to 15°C for 24 h. Figure 2 shows the effect of the growth phase for gene induction on the CDM (g/L), PHB content (% w/w) and levels of insoluble and soluble $PhaC_{A-04}$ protein, comparing *E. coli* JM109 (pColdI-$phaCAB_{A-04}$) and *E. coli* JM109 (pColdTF-$phaCAB_{A-04}$). The $PhaC_{A-04}$ protein was detected by western blot analysis using an anti-His tag antibody as the primary antibody. A band appeared in the western blot at the position corresponding to that of the His-tagged $phaC_{A-04}$ protein (67 kDa) for pColdI-$phaCAB_{A-04}$ and the fusion protein of His-tagged $phaC_{A-04}$ and TF at 115 kDa. By varying the time courses of the growth phase, His-tagged $PhaC_{A-04}$ and the His-tagged $phaC_{A-04}$-TF fusion protein were successfully expressed, with the highest amount of total $phaC_{A-04}$ protein obtained when the $phaCAB_{A-04}$ operon was induced at an OD_{600} of 0.5 (2 h, early exponential phase). The content of soluble $PhaC_{A-04}$-TF fusion protein (Figure 2B, lane 3) in the sample after IPTG induction at an OD_{600} of 0.5 was much higher than that of the $phaC_{A-04}$ protein alone from pColdI-$phaCAB_{A-04}$ (Figure 2A, lane 3), suggesting that the TF chaperone facilitates the expression of highly soluble protein in *E. coli* JM109. Moreover, significant proteolysis of the $PhaC_{A-04}$ protein occurred with pColdI-$phaCAB_{A-04}$ when cells produced a large amount of insoluble $PhaC_{A-04}$ during the exponential phase, resulting in smeared bands of degraded insoluble proteins. On the other hand, proteolysis of the $PhaC_{A-04}$ protein was not observed with pColdTF-$phaCAB_{A-04}$ when cells were induced with 0.5 mM IPTG at an OD_{600} of 0.5. Notably, the highest amount of soluble $PhaC_{A-04}$ and TF fusion protein was produced only at an OD_{600} of 0.5 and was not detected in other growth phases. It was observed that the TF protein could enhance $PhaC_{A-04}$ solubility and prevent $PhaC_{A-04}$ degradation. Functional $PhaC_{A-04}$ protein production was confirmed by determining the amount of PHB produced; however, the value was only 46.57% w/w with a productivity of 0.03 ± 0.01 g/(L·h).

Development of a short-induction method and effect of IPTG concentration on PHB productivity

Next, a short-induction method was investigated in this study with the aim of accelerating growth and PHB production and attaining higher productivity than that afforded by the conventional induction method. The optimization was carried out based on one-factor-at-a-time experiments by varying one factor of interest while keeping other factors constant [37]. First, conditions were optimized by varying the OD_{600} based on cultivation time (0.5, 1.3, 2.1 and 2.4 h) and inducing expression with 0.5 mM IPTG at 15°C for 30 min. Then, the temperature was shifted from 15°C to 37°C for 24 h to enhance growth and PHB production. The effect of the growth phase (OD_{600}) on CDM (g/L) and PHB content (% w/w) is illustrated in Figure 3. Again, it was clearly observed that cells of both *E. coli* JM109 (pColdI-*phaCAB*$_{A-04}$) and *E. coli* JM109 (pColdTF-*phaCAB*$_{A-04}$) in the 2-h early exponential phase (OD_{600} of 0.5) exhibited higher CDM and PHB production than those in other growth phases. After induction with 0.5 mM IPTG at 15°C for 30 min and cultivation at 37°C for 24 h, *E. coli* JM109 (pColdI-*phaCAB*$_{A-04}$) attained 4.5 ± 0.1 g/L CDM, 3.9 ± 0.1 g/L PHB and 85.90 ± 2.6% (w/w) PHB content with a productivity of 0.16 g PHB/(L×h), whereas *E. coli* JM109 (pColdTF-*phaCAB*$_{A-04}$) attained 3.5 ± 0.1 g/L CDM, 2.7 ± 0.1 g/L PHB and 75.90 ± 2.8% (w/w) PHB content with a productivity of 0.11 g PHB/(L×h). Thus, the short-induction method enhanced the PHB content and productivity more than the conventional method. Next, an OD_{600} of 0.5 was used to investigate the optimal concentration of IPTG (0, 0.01, 0.05, 0.1, 0.5, and 1.0 mM) under the short-induction conditions. The effects of various IPTG concentrations on CDM (g/L), PHB (g/L), PHB content (% w/w) and PHB productivity (g PHB/(L×h)), comparing *E. coli* JM109 (pColdI-*phaCAB*$_{A-04}$) and *E. coli* JM109 (pColdTF-*phaCAB*$_{A-04}$), are summarized in Table 2. It can be concluded that the optimal concentration of IPTG was 0.5 mM in both cases. The PHB content (% w/w) increased in accordance with the IPTG concentration, but the amount of PHB (g/L) produced was maximum under induction with 0.5 mM IPTG. The PHB content (% w/w) increased approximately 8-fold, and the productivity (g PHB/(L×h)) increased 16-fold, compared with those under the control condition in the case of pColdI-*phaCAB*$_{A-04}$.

Development of a preinduction method and effect of inoculum size on PHB productivity

We also investigated a preinduction strategy to enhance PHB productivity by extending the PHB production phase at 37°C for an additional 24 h after conventional induction. When the OD_{600} reached 0.5, IPTG was added at 0.5 mM into the culture, and the temperature was reduced from 37°C to 15°C. Then, cultivation was performed for 24 h to allow full expression of the phaCAB$_{A-04}$ protein. Concurrently, the effect of inoculum size (1, 5 and 10% (v/v)) of induced cells was investigated under the preinduction conditions. The results are shown in comparison with those of the conventional induction and short-induction methods (Table 3). The preinduction method with a 5% (v/v) inoculum gave a higher amount of PHB (1.9 ± 0.6 g/L) than conventional induction with an inoculum size of 5% (v/v) (0.6 ± 0.1 g/L) and could extend the productivity of 0.039 ± 0.01 g PHB/(L×h) for 48 h so that the PHB content increased from 46.2 ± 3.8% (w/w) to 67.9 ± 4.8% (w/w). The increase in PHB content and PHB productivity occurred with an increase in the inoculum size. Nevertheless, the short-induction method with an inoculum size of 5% (v/v) gave the highest levels of PHB content and productivity. Therefore, the short-induction method using *E. coli* JM109 (pColdI-*phaCAB*$_{A-04}$) with an inoculum size of 0.5% (v/v) and cultivated until the OD_{600} reached 0.5 (2 h) before induction with 0.5 mM IPTG was selected to investigate the effect of induction temperature in the subsequent experiment.

Effect of induction temperature on PHB productivity

The optimal short-induction temperature was investigated in a range between 15°C and 37°C for 30 min before increasing the temperature to 37°C for 24 h to confirm that the high PHB productivity resulting in this study is a result of the cold-shock cspA promoter and that 15°C is the optimal induction temperature. Figure 4 shows the results of the effect of the short-induction temperature (15, 25, 30 and 37°C) on cell growth and PHB production. It was clear that 15°C was the optimal induction temperature for enhancing the amount of PHB produced, which resulted in a maximum PHB content of 86.2 ± 2.6% (w/w). The amount of PHB produced decreased as the induction temperature increased, with a concomitant increase in RCM. The cold-shock temperature promoted PHB production and suppressed RCM. The PHB productivity at 15°C was 7-fold higher than that obtained with an induction temperature of 37°C.

Effect of cold-shock cspA promoter and TF chaperone on phaCAB$_{A-04}$ and PHB production

In *phaCAB*$_{A-04}$-overexpressing *E. coli* JM 109 (pColdI-*phaCAB*$_{A-04}$) under the conventional conditions, the formation of inclusion bodies of PhaC$_{A-04}$ has been observed due to the low aqueous solubility of the protein, as described previously [32]. To verify that the cold-shock cspA promoter works together with the TF chaperone to improve the solubility of PhaC$_{A-04}$, the hydrophilic GST tag was fused to the N-terminus of PhaC$_{A-04}$ (pGEX-6P-1-*phaCAB*$_{A-04}$), and the effect of the GST tag at 37°C on the polymerization reaction of phaC$_{A-04}$ based on the amount of PHB production was investigated. In addition, pBAD/Thio-TOPO- *phaCAB*$_{A-04}$, encoding a hydrophilic N-terminal thioredoxin fusion protein and C-terminal 6His-fusion protein induced by arabinose, was also used for comparison. The control strain, harboring pUC19-nativeP-*phaCAB*$_{A-04}$, was under the control of the native promoter derived from *C. necator* strain A-04, and no induction agent was required under the same conditions. The amount of PHB produced together with the molecular weight of PHB as a result of *in vivo* polymerization activity are shown in Figure 5A and Table 3. The expressed phaC$_{A-04}$ protein was also verified, purified and quantified and shown in Figure 5B-C and Table 4. From Figure 5A, it was clearly found that pColdI-*phaCAB*$_{A-04}$ and pColdTF-*phaCAB*$_{A-04}$ yielded significantly higher amounts of PHB under the short-induction (15°C for 30 min and then 37°C) conditions than under the conventional induction (15°C) conditions (pColdI-*phaCAB*$_{A-04}$, pColdTF-*phaCAB*$_{A-04}$, pGEX-6P-1-*phaCAB*$_{A-04}$, pBAD/Thio-TOPO-*phaCAB*$_{A-04}$ and pUC19-nativeP-*phaCAB*$_{A-04}$). Next, the expression level of PhaC$_{A-04}$ protein was investigated by SDS-PAGE analysis. Figures 5B and 5C showed insoluble and soluble PhaC$_{A-04}$ expressed at 24 h of cultivation, respectively. The thioredoxin-tagged PhaC$_{A-04}$ fusion protein (lane 2 at 77 kDa) showed the highest amount of insoluble form, corresponding with a low amount of PHB production. The PHB production from pUC19-nativeP-*phaCAB*$_{A-04}$ (Figure 5A)

showed a low amount of PHB similar to that of pGEX-6P-1-*phaCAB*$_{A-04}$ and pBAD/Thio-TOPO-*phaCAB*$_{A-04}$. Interestingly, pColdI-*phaCAB*$_{A-04}$ and pColdTF-*phaCAB*$_{A-04}$ produced significantly high amounts of phaC$_{A-04}$ under both the short and conventional induction methods (Figure 5B lanes 4-7). To clarify and carefully compare the amounts of soluble phaC$_{A-04}$ expressed by pColdI-*phaCAB*$_{A-04}$ and pColdTF-*phaCAB*$_{A-04}$ under short induction and conventional induction, the phaC$_{A-04}$ protein was purified by IMAC affinity chromatography under native conditions. The eluted fractions were quantified by Bradford protein assay. The results are summarized in Table 4. The figures of SDS-PAGE and Western blot analysis were represented as supplementary results. The initial protein loading was adjusted to 2,000 µg and the maximum capacity of the IMAC column was 3,000 µg. The protein recovery was within the range of 90-97%. The conventional method induced soluble phaC$_{A-04}$ from pColdTF-*phaCAB*$_{A-04}$ at a level of as high as 47.4 % of total protein and pColdTF-*phaCAB*$_{A-04}$ enhanced soluble protein formation to approximately 3.09 - 4.1 times higher than that from pColdI-*phaCAB*$_{A-04}$ by both conventional method and short induction method. Based on our observations, the cold-shock cspA promoter enhanced phaC$_{A-04}$ protein expression and TF promoted soluble phaC$_{A-04}$ protein (Figure 5C and Table 4). However, considering the amount of produced PHB from pColdI-*phaCAB*$_{A-04}$ and pColdTF-*phaCAB*$_{A-04}$, Figure 5A, the conventional induction method produced a lower amount of PHB than that obtained from the short method, which was caused by lowered temperature attenuating the metabolic pathway and energy source needed for PHB biosynthesis. The PHB production from pGEX-6P-1-*phaCAB*$_{A-04}$, pBAD/Thio-TOPO-*phaCAB*$_{A-04}$ and pUC19-nativeP-*phaCAB*$_{A-04}$ was not different, which may be attributed to the host strain and induction method used in this study. From Figure 5A, it was distinctly observed that the amounts of PHB produced from pColdTF-*phaCAB*$_{A-04}$ and pColdI-*phaCAB*$_{A-}$04 with the short induction method were significantly higher and produced more rapidly versus the conventional method. Therefore, pColdTF-*phaCAB*$_{A-04}$ and pColdI-*phaCAB*$_{A-}$04 were chosen to validate their effectiveness of PHB production in the 5 L fermenter.

Comparison of PHB production between pColdI-*phaCAB*$_{A-04}$ and pColdTF-*phaCAB*$_{A-04}$ in a 5-L fermenter by the short-induction method

Altogether, for flask cultivation, the optimal conditions were the short-induction method using an inoculum of 0.5% (v/v) in a culture with an OD_{600} of 0.5, cold shock induced with 15°C for a short time, 30 min, and the addition of 0.5 mM IPTG. These conditions were selected as optimal parameters for scaling up production in a 5-L fermenter. The comparison between pColdI-*phaCAB*$_{A-04}$ and pColdTF-*phaCAB*$_{A-04}$ in a 5-L fermenter by the short-induction method was performed because the ratio of the soluble fraction and inclusion bodies of the phaC$_{A-04}$ protein may affect PHB productivity and molecular weight distribution as reported by Harada et al. [32].

Figure 6 shows the time courses of CDM (g/L), RCM (g/L), PHB (g/L), PHB content (% w/w), glucose (g/L), dissolved oxygen (%) and pH during batch cultivation in a 5-L fermenter, comparing *E. coli* JM109 (pColdI-*phaCAB*$_{A-04}$) (Figure 6A) and *E. coli* JM109 (pColdTF-*phaCAB*$_{A-04}$) (Figure 6B). The soluble PhaC$_{A-04}$ protein detected by western blot analysis was also monitored at 6-h intervals over 48 h. The results shown in Table 5 demonstrated that *E. coli* JM109 (pColdTF-*phaCAB*$_{A-04}$) was a more effective PHB producer than the other strain. A PHB content of 90.0±2.3% (w/w), PHB production of 7.9±0.7 g/L, CDM production of 8.8±0.5 g/L, $Y_{P/S}$ value of 0.38 g PHB/g glucose and productivity of 0.43 g PHB/(L×h) were the maximum values obtained using pColdTF-*phaCAB*$_{A-04}$, whereas a PHB content of 78.0±2.1% (w/w), PHB production of 5.8±0.1 g/L, CDM production of 7.2±0.3 g/L, $Y_{P/S}$ value of 0.32 g PHB/g glucose and productivity of 0.24 g PHB/(L×h) were attained using pColdI-*phaCAB*$_{A-04}$. The phaC$_{A-04}$ protein produced by pColdTF-*phaCAB*$_{A-04}$ was more stable and longer lasting (Figure 6B) than that obtained from pColdI-*phaCAB*$_{A-04}$, which was no longer detectable after 30 h of cultivation (Figure 6A). Therefore, we report here that the short-induction strategy facilitates cold shock cspA and chaperone TF proteins to act synergistically to improve the stabilization of PhaC$_{A-04}$ and enhance productivity by 190% and the $Y_{P/S}$ value by 20% in comparsion with the use of cspA alone in pColdI.

Comparison of the molecular weight and thermal and mechanical properties of PHB produced by pColdI-*phaCAB*$_{A-04}$ and pColdTF-*phaCAB*$_{A-04}$ from glucose and crude glycerol

The PHB thin films were subjected to thermal analysis by DSC, molecular weight determination by GPC and mechanical property analysis by a universal testing machine as per the ASTM: D882-91 protocol (Table 5). The PHB from *E. coli* JM109 (pColdI-*phaCAB*$_{A-04}$) had an M_w of 8.17×10^5 Da, an M_n of 1.97×10^5 Da and a PDI of 4.1, whereas the PHB from *E. coli* JM109 (pColdTF-*phaCAB*$_{A-04}$) had an M_w of 2.6×10^5 Da, an M_n of 0.95×10^5 Da and a PDI 2.8, when glucose was used as a carbon source. However, the PHB from *E. coli* JM109 (pColdI-*phaCAB*$_{A-04}$) obtained using crude glycerol had the lowest M_w of 2.42×10^5 Da, an M_n of 0.89×10^5 Da and a PDI of 2.92. Interestingly, the PHB from *E. coli* JM109 (pUC19-nativeP-*phaCAB*$_{A-04}$) obtained using crude glycerol showed the highest M_w of 1.1×10^6 Da, an M_n of 2.6×10^5 Da and a PDI of 4.1. The melting temperature, T_m, of all the PHB film samples produced in this study was in the range of 165-178°C [38], and the glass transition temperature, T_g, was in the normal range of 1-4°C [35, 39, 40]. The Young's modulus and tensile strength of the PHB from *E. coli* JM109 (pColdTF-*phaCAB*$_{A-04}$) possessed the highest values of 5465 MPa and 56.2 MPa, respectively. Figure 6 shows the morphology and transparency of PHB films produced by *C. necator* strain A-04, *E. coli* JM109 (pColdI-*phaCAB*$_{A-04}$) and *E. coli* JM109 (pColdTF-*phaCAB*$_{A-04}$). Interestingly, the PHB films prepared by the film casting technique and produced from *E. coli* JM109 (pColdTF-*phaCAB*$_{A-04}$) showed a soft morphology with high transparency, which was different from the properties of the other PHB films. The PHB films were also subjected to ^{1}H-NMR and ^{13}C-NMR analyses and showed only chemical shifts of the PHB structure.

Discussion

Since 1988, it has been reported that PhaC$_{Re}$, as a type I synthase and the most intensively studied of these proteins, preferentially catalyzes the polymerization of short-chain (R)-hydroxyalkanoic acids (4 to 6 carbon atoms), particularly the conversion of (R)-3-hydroxybutyrate-coenzyme A

(3HBCoA) to poly(3-hydroxybutyrate) (PHB) [20, 27]. In fact, a high concentration of PHB (157 g/L) has been achieved from glucose in high-cell-density cultures of recombinant *E. coli* harboring *phaCAB*$_{Re}$ and the additional cell division protein ftsZ gene [41, 42]. Ultrahigh-molecular-weight PHB and its applications have also been reported by many research groups [15, 22, 43, 44]. PhaC$_{Re}$ has been popularly used to prepare chimeric enzymes to increase its ability to incorporate MCL monomers for SCL-co-MCL production [45].

Beyond these previous reports, there have been few reports on the application of cold-shock systems for PHB production to address the challenges of soluble and functional phaC expression in *E. coli*. One of the attempts was the use of pCold and a GST-fusion tag to obtain pCold-*PhaC*$_{Re}$ and pCold-GST-*PhaC*$_{Re}$, which were overexpressed in *E. coli* DH5α and *E. coli* BL21(DE3) to investigate the effect of GST fusion on the *in vivo* solubility of PhaC$_{Re}$, but the pGEM-T derivative carrying the *pha*$_{Re}$ promoter, His-fused *phaC*$_{Re}$, *phaA*$_{Re}$, and *phaB*$_{Re}$ and pGEM-GST*phaC*$_{Re}$*AB* were used to evaluate *in vitro* PHB production [32]. It was revealed that most of the PhaC$_{Re}$ and GST-PhaC$_{Re}$ when overexpressed in *E. coli* BL21(DE3) were detected in the insoluble fraction rather than the soluble fraction, indicating that the solubility of PhaC$_{Re}$ is not improved by GST tag fusion under a cold-inducible promoter. Another recommendation was that a fusion protein to assist in phaC solubilization as well as the 6His-tag should be fused at the N-terminus of phaC because an N-terminal tag has a weaker effect than a C-terminal tag on the polymerization activity of phaC [30, 32, 46].

Although *C. necator* strain A-04 exhibits 99.78% similarity of 16S rRNA, 99.9% similarity of *phaC*$_{A-04}$ and 100% similarity of *phaA*$_{A-04}$ and *phaB*$_{A-04}$ with those of *C. necator* H16, we observed differences in PHB productivity as well as the monomeric composition of the copolymers and terpolymers when we used the same carbon source [33, 35, 36]. Interestingly, *C. necator* strain A-04 also exhibited different growth abilities on pure glycerol as well as crude glycerol from a biodiesel plant in Thailand as compared with *C. necator* strain H16 (unpublished observations from personal communication with Dr. Tuck Seng Wong, University of Sheffield, United Kingdom). Thus, *C. necator* strain A-04 can be considered as one of the most promising candidates for PHA production at low cost. However, the PHA productivity of *C. necator* strain A-04 still does not meet the requirement for industrial production. Thus, our objective was to investigate the ability of the phaCAB$_{A-04}$ gene operon when heterologously expressed in recombinant *E. coli*. We initially aimed to use the pColdI and pColdTF expression systems to address the challenges of soluble and functional phaC$_{A-04}$ expression in *E. coli* JM109 from glucose and finally evaluate its ability to use crude glycerol as a carbon source for PHB production in a 5-L fermenter to attain low cost PHB production. We also investigated the optimal expression conditions and finally compared them with those for other promoters, including the pGEX-6P-1 derivative, carrying N-terminal GST and 6His-fused *phaCAB*$_{A-04}$; the pBAD/Thio-TOPO derivative, carrying C-terminal 6His- and N-terminal thioredoxin-fused *phaCAB*$_{A-04}$; and pUC19, using a native promoter from *C. necator* strain A-04, in both flask cultivation and the 5-L fermenter. The produced PHB was extracted, purified, and prepared using the glass casting method, and subjected to molecular weight analysis and thermal and mechanical property determination to determine the effect of the cold-shock cspA promoter and TF on the functional expression of phaC$_{A-04}$ and PHB products.

First, this study aimed to solubilize PhaC$_{A-04}$ by using the cold-shock cspA promoter and TF to achieve a high yield of soluble recombinant PhaC$_{A-04}$ from *E. coli* JM109. His-tagged phaC$_{A-04}$ was overexpressed by pColdI, but most of the protein was present in insoluble form, with significant aggregation resulting in smear bands (Figure 2A, 5B and Table 4), whereas the His-tagged phaC$_{A-04}$-TF fusion protein was expressed from pColdTF at lower levels than the protein from pColdI, but most of this protein was present in soluble form (Figures 2B, 5B and Table 4). The ratio of soluble fraction to the total phaC$_{A-04}$ proteins from pColdTF-*phaCAB*$_{A-04}$ was about 3-4 times higher than that from pColdI-*phaCAB*$_{A-04}$ both under short induction and conventional induction method. Thus, it can be concluded that the TF chaperone helped solubilize phaC$_{A-04}$ in our investigation, but PHB production and $Y_{P/S}$ in both systems, namely, pColdI-*phaCAB*$_{A-04}$ and pColdTF-*phaCAB*$_{A-04}$, were not significantly different. To produce PHB using microbial cells under *in vivo* conditions, *phaC* will always naturally be expressed in two forms, namely, insoluble and soluble, and only soluble proteins work under *in vivo* conditions to perform PHB polymerization [32, 47]. Thus, in this study, PhaC$_{A-04}$ was purified, quantified, carefully compared versus pColdI-*phaCAB*$_{A-04}$ and pColdTF-*phaCAB*$_{A-04}$, and also between short induction and conventional induction methods (Table 4 and Figure S1). We also consider the amount of PHB, $Y_{P/S}$, PHB productivity and molecular weight distribution as indirect indicators of PhaC$_{A-04}$ activity because there have been many reports that have gained insights into PhaC$_{Re}$ expression and PHB production that can be used to support our findings. Focusing on chaperone-assisted PhaC$_{Re}$ expression and PHB production, it was previously reported that the TF chaperone (without the cold-shock cspA promoter) was investigated in combination with three chaperone systems for coexpression with PhaC$_{Re}$: GroEL/GroES (plasmid pGro7), TF (plasmid pTf16) and DnaK/DnaJ/GrpE (plasmid pKJE7). Additionally, TF and GroEL/GroES were expressed together (plasmid pG-Tf2), as were GroEL/GroES and DnaK/DnaJ/GrpE (plasmid pG-KJE8) [30]. The study concluded that with the set of strains expressing the N-terminal 6His-tagged fusion protein, the GroEL/GroES system resulted in approximately 6-fold-greater enzyme yields than that obtained in the absence of coexpressed chaperones, whereas TF resulted in approximately 3-fold increases in the soluble protein yield. It seemed likely that although the overexpression of phaC$_{A-04}$ was achieved both in terms of quantity (pColdI) and solubility (pColdTF), its function had already reached its limit, so improvement of PHB production was not further observed. Acceleration of PHB productivity would be another goal for reducing the time consumed for microbial cultivation. It was reported that optimization of expression conditions, including inducer concentrations, age of bacterial cells (OD_{600}) and induction temperatures, is required to improve PHB productivity.

It was reported that the production level of PhaC was not significantly changed by the addition of IPTG at concentrations greater than 0.1 mM, suggesting that this IPTG concentration is sufficient for pJRDTrc*phaCAB*$_{Re}$ to fully express PhaC [31]. In our study, 0.5 mM was the optimal concentration of IPTG for overexpression of phaC$_{A-04}$ under the cold-shock cspA promoter, consistent with a previous report [16]. Cells at the initial exponential phase exhibited the highest phaC$_{A-04}$ expression level, resulting in enhanced PHB productivity under the short-induction method. We also performed parallel experiments using different hydrophilic tags, including expression via the native promoter of *C. necator* strain A-04, N-terminal GST-fused *phaCAB*$_{A-04}$, and N-terminal thioredoxin-fused and C-terminal 6His-fused *phaCAB*$_{A-04}$, to confirm that the high efficiency of PHB production was

contributed by the cold-shock cspA promoter. It was found that N-terminal GST-fused *phaCAB*$_{A-04}$, N-terminal thioredoxin-fused and C-terminal 6His-fused *phaCAB*$_{A-04}$ and expression via the native promoter of *C. necator* strain A-04 gave similar values for CDM production (~ 1.0 g/L), PHB production (~0.8 g/L) and PHB content (~ 65 wt%), which were 2.5 times lower than the values obtained with pCold and pColdTF. Thus, our finding also confirmed that GST-PhaC$_{A-04}$ did not improve PHB production and exhibited lower PHB productivity (longer time of polymerization) than the control pUC19-nativeP-*phaCAB*$_{A-04}$, as previously mentioned by Harada et al. [32]. The *araBAD* promoter and N-terminal thioredoxin-fused *phaCAB*$_{A-}$04 together with C-terminal 6His-fused *phaCAB*$_{A-}$04 showed the highest level of PhaC$_{A-04}$ protein production, but most of them were in insoluble form, resulting in similar effects on PHB production with pGEX-6P-1-*phaCAB*$_{A-04}$ and pUC19-nativeP-*phaCAB*$_{A-04}$. However, *E. coli* JM109 (pGEX-6P-1-*phaCAB*$_{A-04}$) exhibited higher PHB production than that of pGEM-GST*phaC*$_{Re}$*AB* reported previously [32].

It is still unclear why *E. coli* JM109 (pColdI-*phaCAB*$_{A-04}$) and *E. coli* JM109 (pColdTF-*phaCAB*$_{A-04}$) exhibited higher PHB production and productivity than *E. coli* JM109 (pGEX-6P-1-*phaCAB*$_{A-04}$), *E. coli* JM109 (pBAD/Thio-TOPO-*phaCAB*$_{A-04}$) and *E. coli* JM109 pUC19-nativeP-*phaCAB*$_{A-04}$. The results of SDS-PAGE analysis shown in Figure 5B suggested that when PhaC$_{A-04}$ was overexpressed in *E. coli*, the major fraction was presented in insoluble form [32]. In addition, this may be because the use of different genetic constructs (e.g. different promoters) changes the respective PhaA and PhaB expression resulting in different PHB productivity obtained under different promoters. Although the conventional induction method at 15°C resulted in soluble PhaC$_{A-04}$ protein content of as high as 47.4 ± 2.4% of total protein, and 3 times higher than the short induction method, the PHB productivity, specific growth rate and specific production rate were much slower and lower than for the short induction method. Thus, the short induction method may be more practical than the conventional method in large scale production. Finally, the production of PHB of pColdI-*phaCAB*$_{A-04}$ and pColdTF-*phaCAB*$_{A-04}$ was compared in the 5-L fermenter for the under short induction method. The produced PHB were characterized and it was found that the M_w of PHB produced from pColdTF-*phaCAB*$_{A-04}$, for which soluble phaC$_{A-04}$ was 4.1 times higher than pColdI-*phaCAB*$_{A-04}$ was lower than that from pColdI-*phaCAB*$_{A-04}$. Hiroe et al. have reported that the relative amounts of PhaA, PhaB and PhaC affect PHB production [15]. They also concluded that the concentration of active PHA synthase had a negative correlation with PHB molecular weight and a positive correlation with cellular PHB content, similar to our observation. The M_w and M_n of PHB produced by pColdTF were lower than those of pColdI-*phaCAB*$_{A-04}$ and pUC19-nativeP-pha*CAB*$_{A-04}$. In this case, TF increases PhaC production and its Mw decreases due to the presence of more active PhaC.

To achieve low-cost production, crude glycerol as a byproduct from biodiesel production was used as a carbon source to produce PHB using pColdI-*phaCAB*$_{A-04}$ and pUC19-nativeP-pha*CAB*$_{A-04}$. With *E. coli* JM109 (pColdI-*phaCAB*$_{A-04}$), PHB produced from crude glycerol had an M_w of 2.42×10^5 Da and an M_n of 0.89×10^5 Da with a PDI of 2.92, whereas those results from glucose were M_w of 8.41×10^5 Da and an M_n of 2.03×10^5 Da with a PDI of 4.14. In addition, the PHB content and productivity from crude glycerol were also lower than those obtained from glucose. Typically, PHB obtained from glycerol was reported to have a significantly lower molecular weight than polymers synthesized from other substrates, such as glucose or lactose [48, 49]. It has been concluded that M_n of PHB produced by *C. necator* NCIMB 40529 from glycerol was substantially lower than for PHB produced from glucose because a glycerol molecule bound to the PHB chain via the primary or secondary hydroxyl groups. Subsequently, a primary hydroxyl group of glycerol is involved in chain transfer, which is a random transesterification process and PHA synthase does not catalyze chain transfer. It has been proposed that the end-group structure produced by chain transfer to a primary hydroxyl of glycerol is the preferred reaction. Conversely, end-group analysis of PHB produced from glucose consistently detected only carboxyl end-groups. Thus, it has been concluded that the termination step involves a chain transfer (CT) reaction in which the polymer chain is transferred to a CT agent. A number of possible CT agents have been proposed, including 3HB-CoA [50], water [9], CT agent activated by water [51] or glycerol [48]. Each of the compounds that caused a reduction in the M_n of PHB possesses at least one hydroxyl group.

In our study, when pColdI-*phaCAB*$_{A-04}$-expressing *E. coli* was used to produce PHB from crude glycerol and compared with pUC19-nativeP-*phaCAB*$_{A-04}$-expressing *E. coli*, although the amounts of PHB were similar, an M_w of 1.1×10^6 Da, an M_n of 2.6×10^5 Da and a PDI of 4.1 were obtained from pUC19-nativeP-*phaCAB*$_{A-04}$-expressing *E. coli,* indicating that slow and low phaC$_{A-04}$ expression prolonged and maintained the phaC$_{A-04}$ polymerization activity [15]. It was observed that high levels of phaC proteins resulted in high levels of PHB production, but the chain termination reaction of PhaC polymerization activity frequently occurred faster than that observed with slowed and low expression of the PhaC$_{A-04}$ protein under pUC19-nativeP-*phaCAB*$_{A-04}$, which in turn resulted in a low amount of PHB with a high molecular weight. In the latter case, the low-level phaC protein slowly utilized the substrate, 3-hydroxybutyric-CoA, via a low-competition reaction with other phaC proteins. The benchmark results are shown in Table 6.

Conclusion

This study aimed to improve functional PhaC$_{A-04}$ expression levels in *E. coli* JM109 and found that the cspA promoter in a cold-inducible vector can enhance total PhaC$_{A-04}$ expression and TF chaperones showed obvious effects on enhancing PhaC solubility. However, the ratio of soluble to total PhaC$_{A-04}$ proteins did not play an important role in PHB productivity. The high level of phaC$_{A-04}$ resulted in a high PHB amount, but the chain termination reaction of PhaC polymerization occurred faster than that with the slowed and low expression of phaC$_{A-04}$ by pUC19-nativeP-*phaCAB*$_{A-04}$, which resulted in a low PHB amount with a high molecular weight. The findings suggest that although glycerol which is a CT agent was used as a carbon source, PHB produced by pUC19-nativeP-*phaCAB*$_{A-04}$ still undergoes chain elongation, and high-molecular-weight PHB is obtained.

Materials And Methods

Strains and plasmids

The *E. coli* strains and plasmids used in this study are listed in Table 1. The PHB-producing *C. necator* strain A-04 [52] was used to isolate the phaCAB$_{A-04}$ gene operon. All bacterial strains were grown at 37°C in Luria-Bertani (LB) medium supplemented with 100 mg/L ampicillin. The LB medium contained (per liter) 10 g of tryptone (Himedia, Mumbai, India), 5 g of yeast extract (Himedia, Mumbai, India) and 10 g of NaCl (Merck KGaA, Darmstadt, Germany). Stock cultures were maintained at -80°C in a 15% glycerol solution. The experiments were performed in a biosafety level 1 laboratory and by researchers and investigators who had undergone biosafety training.

Construction of recombinant plasmids

The *phaCAB* $_{A-04}$ operon PHB biosynthetic genes from *C. necator* A-04 were PCR-amplified using the following pair of primers: forward primer 5'-ATGGATCCCTCGAGATGGCGACCGGCAAAG-3' (the XhoI site is underlined) and reverse primer 5'-GTGAATTCAAGCTTTCAGCCCATATGCAGGCC-3' (the HindIII site is underlined). Primers were designed based on accession numbers FJ897463, FJ897461 and FJ897462. The blunted PCR product was purified and subcloned into pBluescript SK− (Stratagene, La Jolla, CA, USA) linearized by SmaI. The recombinant plasmid digested with XhoI and HindIII was cloned into cold-shock-inducible pColdI and pColdTF vectors (Takara Bio Inc., Shiga, Japan) at the XhoI and HindIII restriction sites, yielding pColdI-phaCAB$_{A-04}$ and pColdTF-phaCAB$_{A-04}$, respectively. For the plasmid pGEX-6P-1-phaCAB$_{A-04}$, the phaCAB$_{A-04}$ operon was amplified by the primers pGEX-F and pGEX-R (Table 1). The 3,885-bp DNA fragment was digested by BamHI and XhoI and cloned into BamHI-XhoI-digested pGEX-6P-1 to obtain pGEX-6P-1-*phaCAB*$_{A04}$. To construct pUC19-nativeP-phaCAB$_{A-04}$, the primers nativeP-*phaCAB*$_{A-04}$-F and nativeP-*phaCAB*$_{A-04}$-R were used to amplify the *phaCAB*$_{A-04}$ operon, including its native promoter. The blunted PCR product was purified and cloned into SmaI-linearized pUC19 (Thermo Fisher Scientific, Inc., Waltham, MA, USA), yielding pUC19-nativeP-*phaCAB*$_{A-04}$. PCRs were performed using Q5® High-Fidelity DNA Polymerase (New England Biolabs, Ipswich, MA, USA). *E. coli* JM109 was used as a host for cloning and PHB production. The accuracy of the constructed plasmid was verified by the corresponding restriction enzyme and sequencing.

Optimization of culture conditions for PHB production in shake flask cultivation

Expression vectors named pColdI-*phaCAB*$_{A-04}$ and pColdTF-*phaCAB*$_{A-04}$ with the entire phaCAB$_{A-04}$ operon were transformed into *E. coli* JM109 by the heat shock method [53]. Shake flask experiments were performed in 250-mL Erlenmeyer flasks containing 50 mL of medium. *E. coli* JM109 cells transformed with pColdI-*phaCAB*$_{A-04}$ or pColdTF-*phaCAB*$_{A-04}$ were grown in LB medium containing ampicillin (100 μg/mL) on a rotary incubator shaker (Innova 4300, New Brunswick Scientific Co., Inc., Edison, NJ, USA) at 37°C and 200 rpm for 24 h. The overnight seed culture was inoculated into fresh LB medium (5% v/v inoculum) containing 100 mg/L ampicillin and 20 g/L glucose prior to induction with temperature and IPTG using three separate induction methods (Figure 1).

For the synthesis of PHB using the conventional induction method, the procedure was performed according to the user manual (Takara Bio Inc., Otsu, Shiga, Japan). The culture was incubated at 37°C and 200 rpm until the optical density at 600 nm (OD_{600}) reached 0.5, 1.3, 2.1 and 2.4. Next, the cultivation temperature was reduced from 37°C to 15°C for 30 min. The expression of the *phaCAB* operon was induced by the addition of 0.5 mM IPTG, and cultivation was continued at 15°C for an additional 24 h.

For the synthesis of PHB using the short-induction method developed in this study, the culture was incubated at 37°C and 200 rpm until the OD_{600} reached 0.5, 1.3, 2.1 and 2.4. Then, the temperatures were varied at 15, 25, 30 and 37°C for 30 min. Next, the expression of the *phaCAB* operon was induced by adding various concentrations (0.01, 0.05, 0.1, 0.5 and 1.0 mM) of IPTG, and the cultivation was maintained at 37°C for 24 h.

For the synthesis of PHB using the preinduction method developed in this study, the culture was incubated at 37°C and 200 rpm until the OD_{600} reached 0.5. Then, 0.5 mM IPTG was added to the culture and the temperature was reduced from 37°C to 15°C for 24 h. The induced cells were harvested by centrifugation, the medium was discarded, and the cells were resuspended in an equal volume of fresh LB medium. Then, the induced cells at 1, 5 or 10% (v/v) were transferred into fresh LB medium supplemented with 100 mg/L ampicillin and 20 g/L glucose and incubated at 37°C and 200 rpm for 24 h.

For comparison of the effect of phaC expression on PHB production under various types of promoters, fusion proteins and chaperones, shake flask experiments were performed in 250-mL Erlenmeyer flasks containing 50 mL of LB medium containing ampicillin (100 μg/mL) on a rotary incubator shaker at 37°C and 200 rpm for 24 h. For PHB production, overnight cultures in LB medium (1 mL) were transferred into fresh LB medium supplemented with glucose (20 g/L) and ampicillin (100 μg/mL). Recombinant *E. coli* JM109 (pColdI-*phaCAB*$_{A-04}$) and *E. coli* JM109 (pColdTF-*phaCAB*$_{A-04}$) were induced to produce PHB using the conventional induction method and short-induction method. The effect of GST (the hydrophilic fusion protein) and the tac promoter on PHB production was investigated using *E. coli* JM109 (pGEX-6P-1-*phaCAB*$_{A-04}$), which was induced by the addition of IPTG (0.5 mM). The effect of the araBAD promoter and N-terminal thioredoxin fusion protein together with the C-terminal 6His-fusion protein on PhaC and PHB production was examined by inducing *E. coli* JM109 (pBAD/Thio-TOPO-*phaCAB*$_{A-04}$) with arabinose (1% w/v). *E. coli* JM109 (pUC19-nativeP-*phaCAB*$_{A-04}$), which exhibits expression from native promoter without addition of IPTG, was used as a control strain. All of these comparison experiments were performed at 15°C or 37°C for 48 h.

Conditions for PHB production in a 5-L fermenter

A preculture was prepared in 500-mL Erlenmeyer flasks containing 100 mL of LB medium and grown on a rotary shaker at 37°C at 200 rpm for 24 h. The preculture was inoculated into a 5-L bioreactor (MDL500, B.E. Marubishi Co., Ltd., Tokyo, Japan) containing 2 L of LB medium supplemented with 100 mg/L ampicillin and 20 g/L glucose at an inoculation volume of 5% (v/v). The agitation speed and the air flow rate were 500 rpm and 1 mL/min, respectively. After an OD_{600} of 0.5 was obtained, the cultivation temperature was reduced from 37°C to 15°C for 30 min. Next, IPTG was added to the culture at a final concentration of 0.5 mM. After IPTG addition, the cultivation temperature was shifted from 15°C to 37°C and maintained at 37°C for 48 h. Culture samples were collected at 6 h intervals for 48 h.

Analytical methods

Cell growth was monitored by the CDM, which was determined by filtering 5 mL of the culture broth through preweighed cellulose nitrate membrane filters (pore size = 0.22 mm; Sartorius, Goettingen, Germany). The filters were dried at 80°C for 2 days and stored in desiccators. The net biomass was defined as the residual cell mass (RCM), which was calculated by subtracting the amount of PHB from the CDM. The PHB in dried cells was methyl-esterified using a mixture of chloroform and 3% (v/v) methanol-sulfuric acid (1:1 v/v) [54]. The resulting monomeric methyl esters were quantified by a gas chromatograph (model CP3800, Varian Inc., Walnut Creek, CA, USA) using a Carbowax-PEG capillary column (0.25-mm df, 0.25-mm ID, 60-m length, Varian Inc.). The internal standard was benzoic acid, and the external standard was PHB (Sigma-Aldrich Corp.). The total reducing sugar concentration was determined using a 3,5-dinitrosalicylic acid (DNS) assay [55].

Sodium dodecyl sulfate-polyacrylamide gel electrophoresis (SDS-PAGE) and western blot analysis.

Recombinant *E. coli* cells were cultured with and without induction. Cells were collected by centrifugation at 17,000 ×*g* and 4°C for 30 min. Cell pellets were resuspended in 100 mM Tris-HCl (pH 8.0) and normalized to an OD_{600} of 2.0. Total proteins were extracted from cells by using a sonicator (Sonics Vibra Cell VCX 130, Sonics & Materials, Inc., Newtown, CT, USA). The lysis mixture was then centrifuged at 17,000 ×*g* at 4°C for 30 min. The protein concentration in the supernatant (soluble protein) was estimated by the Bradford method using a Bio-Rad protein assay kit (Bio-Rad Laboratories Inc., Hercules, CA, USA), and bovine serum albumin was used as a standard. Thirty micrograms of total protein from each sample was subjected to sodium dodecyl sulfate-polyacrylamide gel electrophoresis (SDS-PAGE) using 10% polyacrylamide gels under reducing conditions and electrophoresed at 80 V for 10 min followed by 140 V for 60 min. For the western blot analysis, the protein from SDS-PAGE was then transferred to a polyvinylidene difluoride (PVDF) membrane using a semi-dry blotting system (Trans-Blot SD Cell, Bio-Rad Laboratories Inc, Hercules, CA, USA) at 150 mA for 40 min. The 6His tag was detected by a mouse anti-His antibody (Aviva Systems Biology Corp., San Diego, CA, USA) and an HRP-conjugated goat anti-mouse IgG as the primary and secondary antibodies, respectively. Color development was performed using a Mouse IgG DAB Chromogenic Reagent Kit (Boster Biological Technology, Pleasanton CA, USA) according to the manufacturer's instructions.

Protein purification by immobilized metal affinity column

The cell pellet (from 50 mL culture) was resuspended in 1 ml of lysis-equilibration-wash buffer (1X LEW buffer, 50 mM NaH_2PO_4, 300 mM NaCl and pH 8.0). Lysozyme (USB Corporation, OH, USA) and Benzonase® endonuclease (Novagen Inc., WI, USA) were added to concentrations of 0.2 mg/mL and 20 U/mL, respectively. The cells were ruptured by ultrasonic homogenizer (Vibra-Cell™ Ultrasonic Liquid Processors VCX 130, Sonics & Materials, Inc., CT, USA). The amplitude was set to 40% (pulse interval at 30/15 seconds for 5 minutes). The lysate was clarified by centrifugation at 16,100 ×g for 20 minutes and the supernatant was collected. Protino® Ni-IDA 1000 His-Tag Protein purification columns (Macherey-Nagel GmbH & Co. KG, Düren, Germany) were pre-equilibrated with 4 bed volumes of 1X LEW buffer and allowed to drain by gravity. The cleared supernatant with 2 mg of total protein was loaded onto a pre-equilibrated column and washed with 4 bed volumes of 1X LEW buffer containing 20 mM imidazole. Finally, the polyhistidine-tagged protein was eluted with elution buffer (50 mM NaH_2PO_4, 300 mM NaCl, 250 mM imidazole and pH 8.0). Each fraction was analyzed by running 10 µL of eluate on SDS-PAGE and quantified by Bradford protein assay. To ensure accurate quantitation of yields, the lysate flow-through was collected for detection of unbound product by SDS-PAGE analysis.

Analysis of polymer molecular weight

The molecular weight was determined by gel permeation chromatography (GPC; Shimadzu 10A GPC system, Shimadzu Co., Ltd., Kyoto, Japan) with a 10A refractive index detector and two Shodex columns (GPC K-806M columns; 8.0 mm ID × 300 mm L, Showa Denko K.K., Tokyo, Japan). The polymer was dissolved in 0.1% (w/v) chloroform and filtered through a 0.45-µm Durapore® (PVDF) membrane filter with low protein binding capacity (Millex®-HV, Merck Millipore Ltd., Tullagreen, Carrigtwohill Co., Cork, Ireland). The temperature was 40°C, and the flow rate was 0.8 mL/min. A standard curve was determined for polystyrene with low polydispersity under the same conditions for molecular weights of 1.26×10^3, 3.39×10^3, 1.30×10^4, 5.22×10^4, 2.19×10^5, 7.29×10^5, 2.33×10^6 and 7.45×10^6. The M_w and the number-average molecular weight (M_N) were determined by GPC, and the polydispersity index (PDI) was calculated as the ratio:

$\frac{M_w}{M_n}$.

Preparation of PHB films

PHB films were prepared according to the ASTM: D882-91 protocol. The PHB films were prepared from chloroform solutions of the polyesters using conventional solvent-casting techniques and a glass tray (Pyrex, Corning Incorporated, Corning NY, USA) as the casting surface (modified from [56]). The thickness of the thin polyester films was regulated by controlling the concentration of the polymer in chloroform (1% w/v) and the volume of the polymer solution. The thickness of the PHB films was 0.05 mm, which was confirmed using a caliper (Model 500-175: CD-12C, Mitutoyo Corporation, Kawasaki-shi, Kanagawa, Japan). Film samples were aged for 1 month in a desiccator at ambient temperature to allow them to reach crystallization equilibrium.

Analysis of the mechanical properties of PHB films

The mechanical tests were conducted at the Scientific and Technological Research Equipment Center, Chulalongkorn University, using a universal testing machine (H10KM, Wuhan Huatian Electric Power Automation Co., Ltd., Wuhan, China) with a crosshead speed of 10 mm/min. The variables measured included the elongation at the break point (%), the stress at maximal load (MPa), and the Young's modulus (MPa). The data represent the mean values for ten samples tested under the same conditions.

Thermal analysis by differential scanning calorimetry (DSC)

A 10-mg sample of PHB was encapsulated in an aluminum sample vessel and placed in the sample holding chamber of the DSC apparatus (DSC7, PerkinElmer, Inc., Waltham, MA, USA). STAR^e software (version SW 10.00; Mettler-Toledo International Inc., Columbus, OH, USA) was used to operate the DSC apparatus at the Petroleum and Petrochemical College, Chulalongkorn University. The previous thermal history of the sample was removed before the thermal analysis by heating the sample from ambient temperature to 180°C at 10°C/min. Next, the sample was maintained at 180°C for 5 min before cooling at 10°C/min to −50°C. The sample was then thermally cycled at 10°C/min to 180°C. The melting peak temperature, denoted by T_m, was given by the intersection of the tangent with the furthest point of an endothermic peak and the extrapolated sample baseline. The glass transition temperature, denoted by T_g, could be estimated by extrapolating the midpoint of the heat capacity difference between glassy and viscous states after heating of the quenched sample.

Data analysis

All data presented in this manuscript are representative of the results of three independent experiments and are expressed as the mean values ± standard deviations (SDs). One-way analysis of variance (ANOVA) followed by Duncan's test for testing differences among means was conducted using SPSS version 22 (IBM Corp., Armonk, NY, USA). Differences were considered significant at $P < 0.05$.

Future Research Directions

Recently, state-of-the-art technology has been applied in the development of recombinant technologies for PHB production to replace fossil-derived plastics with competitive green technologies for PHB production. Projects are ongoing in our laboratory to develop a technoeconomic platform for PHB production in both wild-type and recombinant strains from sustainable feedstocks such as glycerol waste from the biodiesel industry. Optimization based on high-cell-density cultivation will be conducted in fed-batch cultivation to enhance productivity and shorten cultivation time. The green extraction and purification process developed in previous work will be integrated into this framework. Purified PHB is used in the development of innovative technologies for applications in microbeads and packaging.

Abbreviations

NA: Not Applicable; PHAs: polyhydroxyalkanoates; PHB: poly(3-hydroxybutyrate); CDM: cell dry mass; RCM: residual cell mass; DSC: differential scanning calorimetry; GPC: gel permeation chromatography; : yield coefficient of PHB produced from consumed PHB substrate (g PHB/g PHB substrate); : yield coefficient of the residual cell mass produced from the consumed PHB substrate (g RCM/g PHB substrate)

Declarations

Acknowledgments

This research was supported in part by the 100th Anniversary Chulalongkorn University Fund for Doctoral Scholarship and the 90th Anniversary of Chulalongkorn University (Ratchadapiseksomphot) Endowment Fund. The authors greatly appreciate the support and useful advice from Associate

Professor Takeharu Tsuge at the Department of Materials Science and Engineering, School of Materials and Chemical Technology, Tokyo Institute of Technology, Yokohama, Japan, regarding the analysis of molecular weight distributions by gel permeation chromatography. We also thank Ms. Jittakan Pachimsawat at the Program in Biotechnology, Faculty of Science, Chulalongkorn University, for her contribution to the molecular weight distribution analysis. We would like to thank Bangchak Initiative Innovation Center at Bangchak Corporation Public Company Limited for providing the glycerol wastes used in this study.

Authors' contributions

TB performed the experiments and discussed the results. RWS provided guidance for the experimental design and discussed the results. KH provided suggestions for the experimental design and discussed the results. SCN provided guidance and suggestions for the experimental design, discussed the results, and wrote and revised the manuscript. All authors read and approved the final version of the manuscript.

Funding

This research was supported in part by the 100th Anniversary Chulalongkorn University Fund for Doctoral Scholarship and the 90th Anniversary of Chulalongkorn University (Ratchadapiseksomphot) Endowment Fund.

Availability of data and materials

The PHA biosynthesis operon of *C. necator* strain A-04 consisted of three genes sequences was uploaded

to GenBank® (acetyl-CoA acetyltransferase ($phaA_{A\text{-}04}$, 1182 bp, 40.6 kDa, accession no. FJ897461), acetoacetyl-CoA reductase ($phaB_{A\text{-}04}$, 741 bp, 26.4 kDa, accession no. FJ897462) and PHB synthase ($phaC_{A\text{-}04}$, 1770 bp, 64.3 kDa, accession no. FJ897463).

Ethics approval and consent to participate

Not applicable.

Author details

[1]Department of Microbiology, Faculty of Science, Chulalongkorn University, Phayathai Road, Patumwan, Bangkok 10330, Thailand

[2]International Center for Biotechnology, Osaka University, Osaka University, 2-1 Yamadaoka, Suita, Osaka 565-0871, Japan.

Competing interests

The authors certify that no actual or potential conflicts of interest in relation to this article exist.

Consent for publication

The authors agree to publish in the journal.

References

1. Schnurr RE, Alboiu V, Chaudhary M, Corbett RA, Quanz ME, Sankar K, Srain HS, Thavarajah V, Xanthos D, Walker TR: **Reducing marine pollution from single-use plastics (SUPs): A review.** *Marine pollution bulletin* 2018, **137:**157-171.
2. Prata JC, Silva ALP, Da Costa JP, Mouneyrac C, Walker TR, Duarte AC, Rocha-Santos T: **Solutions and integrated strategies for the control and mitigation of plastic and microplastic pollution.** *International journal of environmental research and public health* 2019, **16:**2411.
3. Xanthos D, Walker TR: **International policies to reduce plastic marine pollution from single-use plastics (plastic bags and microbeads): a review.** *Marine pollution bulletin* 2017, **118:**17-26.
4. Steensgaard IM, Syberg K, Rist S, Hartmann NB, Boldrin A, Hansen SF: **From macro-to microplastics-Analysis of EU regulation along the life cycle of plastic bags.** *Environmental Pollution* 2017, **224:**289-299.
5. Skoczinski RCP, Carus M, Baltus W, Doris de Guzman HK, Raschka A, Ravenstijn J: **Global markets and trends of bio-based building blocks and polymers 2019–2024.** www.bio-based.eu/reports: nova-Institut GmbH; 2019.
6. Gross RA, Kalra B: **Biodegradable polymers for the environment.** *Science* 2002, **297:**803-807.
7. Volova T, Gladyshev M, Trusova MY, Zhila N: **Degradation of polyhydroxyalkanoates in eutrophic reservoir.** *Polymer Degradation and Stability* 2007, **92:**580-586.
8. Lemoigne M: **Études sur l'autolyse microbienne origine de l'acide β-oxybutyrique formé par autolyse.** *Annales de l'Institut Pasteur* 1927, **41:**148.
9. Kawaguchi Y, Doi Y: **Kinetics and mechanism of synthesis and degradation of poly (3-hydroxybutyrate) in *Alcaligenes eutrophus*.** *Macromolecules* 1992, **25:**2324-2329.
10. Gebauer B, Jendrossek D: **Assay of poly (3-hydroxybutyrate) depolymerase activity and product determination.** *Applied and Environmental Microbiology* 2006, **72:**6094-6100.

11. Liu F, Li W, Ridgway D, Gu T, Shen Z: **Production of poly-β-hydroxybutyrate on molasses by recombinant *Escherichia coli*.** *Biotechnology Letters* 1998, **20:**345-348.
12. Ahn WS, Park SJ, Lee SY: **Production of Poly (3-hydroxybutyrate) by fed-batch culture of recombinant *Escherichia coli* with a highly concentrated whey solution.** *Applied and Environmental Microbiology* 2000, **66:**3624-3627.
13. Taguchi K, Taguchi S, Sudesh K, Maehara A, Tsuge T, Doi Y: **Metabolic pathways and engineering of polyhydroxyalkanoate biosynthesis.** *Biopolymers Online: Biology• Chemistry• Biotechnology• Applications* 2005, **3**.
14. Agus J, Kahar P, Abe H, Doi Y, Tsuge T: **Molecular weight characterization of poly [(R)-3-hydroxybutyrate] synthesized by genetically engineered strains of *Escherichia coli*.** *Polymer degradation and stability* 2006, **91:**1138-1146.
15. Hiroe A, Tsuge K, Nomura CT, Itaya M, Tsuge T: **Rearrangement of gene order in the phaCAB operon leads to effective production of ultrahigh-molecular-weight poly [(R)-3-hydroxybutyrate] in genetically engineered *Escherichia coli*.** *Applied and Environmental Microbiology* 2012, **78:**3177-3184.
16. Kahar P, Agus J, Kikkawa Y, Taguchi K, Doi Y, Tsuge T: **Effective production and kinetic characterization of ultra-high-molecular-weight poly [(R)-3-hydroxybutyrate] in recombinant *Escherichia coli*.** *Polymer degradation and stability* 2005, **87:**161-169.
17. Lee SY, Lee KM, Chan HN, Steinbüchel A: **Comparison of recombinant *Escherichia coli* strains for synthesis and accumulation of poly-(3-hydroxybutyric acid) and morphological changes.** *Biotechnology and bioengineering* 1994, **44:**1337-1347.
18. Rehm BH: **Polyester synthases: natural catalysts for plastics.** *Biochemical Journal* 2003, **376:**15-33.
19. Tsuge T: **Fundamental factors determining the molecular weight of polyhydroxyalkanoate during biosynthesis.** *Polymer Journal* 2016, **48:**1051-1057.
20. Schubert P, Steinbüchel A, Schlegel HG: **Cloning of the *Alcaligenes eutrophus* genes for synthesis of poly-beta-hydroxybutyric acid (PHB) and synthesis of PHB in *Escherichia coli*.** *Journal of bacteriology* 1988, **170:**5837-5847.
21. Peoples OP, Sinskey AJ: **Poly-beta-hydroxybutyrate (PHB) biosynthesis in *Alcaligenes eutrophus* H16. Identification and characterization of the PHB polymerase gene (phbC).** *Journal of Biological Chemistry* 1989, **264:**15298-15303.
22. Iwata T: **Strong fibers and films of microbial polyesters.** *Macromolecular bioscience* 2005, **5:**689-701.
23. Wittenborn EC, Jost M, Wei Y, Stubbe J, Drennan CL: **Structure of the catalytic domain of the class I polyhydroxybutyrate synthase from *Cupriavidus necator*.** *Journal of Biological Chemistry* 2016, **291:**25264-25277.
24. Kim J, Kim YJ, Choi SY, Lee SY, Kim KJ: **Crystal structure of *Ralstonia eutropha* polyhydroxyalkanoate synthase C-terminal domain and reaction mechanisms.** *Biotechnology journal* 2017, **12:**1600648.
25. Chek MF, Kim S-Y, Mori T, Arsad H, Samian MR, Sudesh K, Hakoshima T: **Structure of polyhydroxyalkanoate (PHA) synthase PhaC from *Chromobacterium* sp. USM2, producing biodegradable plastics.** *Scientific reports* 2017, **7:**1-15.
26. Gerngross T, Martin D: **Enzyme-catalyzed synthesis of poly [(R)-(-)-3-hydroxybutyrate]: formation of macroscopic granules in vitro.** *Proceedings of the National Academy of Sciences* 1995, **92:**6279-6283.
27. Gerngross T, Snell K, Peoples O, Sinskey A, Csuhai E, Masamune S, Stubbe J: **Overexpression and purification of the soluble polyhydroxyalkanoate synthase from *Alcaligenes eutrophus*: evidence for a required posttranslational modification for catalytic activity.** *Biochemistry* 1994, **33:**9311-9320.
28. Yuan W, Jia Y, Tian J, Snell KD, Müh U, Sinskey AJ, Lambalot RH, Walsh CT, Stubbe J: **Class I and III polyhydroxyalkanoate synthases from *Ralstonia eutropha* and Allochromatium vinosum: characterization and substrate specificity studies.** *Archives of Biochemistry and Biophysics* 2001, **394:**87-98.
29. Zhang S, Yasuo T, Lenz RW, Goodwin S: **Kinetic and mechanistic characterization of the polyhydroxybutyrate synthase from *Ralstonia eutropha*.** *Biomacromolecules* 2000, **1:**244-251.
30. Thomson NM, Saika A, Ushimaru K, Sangiambut S, Tsuge T, Summers DK, Sivaniah E: **Efficient production of active polyhydroxyalkanoate synthase in *Escherichia coli* by coexpression of molecular chaperones.** *Appl Environ Microbiol* 2013, **79:**1948-1955.
31. Agus J, Kahar P, Abe H, Doi Y, Tsuge T: **Altered expression of polyhydroxyalkanoate synthase gene and its effect on poly [(R)-3-hydroxybutyrate] synthesis in recombinant *Escherichia coli*.** *Polymer degradation and stability* 2006, **91:**1645-1650.
32. Harada K, Nambu Y, Mizuno S, Tsuge T: **In vivo and in vitro characterization of hydrophilic protein tag-fused *Ralstonia eutropha* polyhydroxyalkanoate synthase.** *International journal of biological macromolecules* 2019, **138:**379-385.
33. Chanprateep S, Katakura Y, Visetkoop S, Shimizu H, Kulpreecha S, Shioya S: **Characterization of new isolated *Ralstonia eutropha* strain A-04 and kinetic study of biodegradable copolyester poly(3-hydroxybutyrate-co-4-hydroxybutyrate) production.** *Journal of Industrial Microbiology and Biotechnology* 2008, **35:**1205-1215.
34. Visetkoop S: **Cloning and expression of polyhydroxyalkanoate biosynthesis genes from *Ralstonia eutropha* strain A-04 in *Escherichia coli*.** [Master Thesis]. [Bangkok, Thailand] Chulalongkorn University; 2009.
35. Chanprateep S, Buasri K, Muangwong A, Utiswannakul P: **Biosynthesis and biocompatibility of biodegradable poly(3-hydroxybutyrate-co-4-hydroxybutyrate).** *Polymer Degradation and Stability* 2010, **95:**2003-2012.
36. Chanprateep S, Kulpreecha S: **Production and characterization of biodegradable terpolymer poly(3-hydroxybutyrate-co-3-hydroxyvalerate-co-4-hydroxybutyrate) by *Alcaligenes* sp. A-04.** *Journal of Bioscience and Bioengineering* 2006, **101:**51-56.
37. Czitrom V: **One-factor-at-a-time versus designed experiments.** *The American Statistician* 1999, **53:**126-131.

38. Owen A, Heinzel J, Škrbić Ž, Divjaković V: **Crystallization and melting behaviour of PHB and PHB/HV copolymer.** *Polymer* 1992, **33:**1563-1567.
39. Doi Y, Kitamura S, Abe H: **Microbial synthesis and characterization of poly (3-hydroxybutyrate-co-3-hydroxyhexanoate).** *Macromolecules* 1995, **28:**4822-4828.
40. Shimamura E, Scandola M, Doi Y: **Microbial synthesis and characterization of poly (3-hydroxybutyrate-co-3-hydroxypropionate).** *Macromolecules* 1994, **27:**4429-4435.
41. Wang F, Lee SY: **Production of poly (3-hydroxybutyrate) by fed-batch culture of filamentation-suppressed recombinant *Escherichia coli*.** *Applied and Environmental Microbiology* 1997, **63:**4765-4769.
42. Choi J-i, Lee SY: **High level production of supra molecular weight poly (3-hydroxybutyrate) by metabolically engineered *Escherichia coli*.** *Biotechnology and Bioprocess engineering* 2004, **9:**196-200.
43. Kusaka S, Iwata T, Doi Y: **Microbial synthesis and physical properties of ultra-high-molecular-weight poly [(R)-3-hydroxybutyrate].** *Journal of Macromolecular Science, Part A: Pure and Applied Chemistry* 1998, **35:**319-335.
44. Kabe T, Tsuge T, Kasuya K-i, Takemura A, Hikima T, Takata M, Iwata T: **Physical and structural effects of adding ultrahigh-molecular-weight poly [(R)-3-hydroxybutyrate] to wild-type poly [(R)-3-hydroxybutyrate].** *Macromolecules* 2012, **45:**1858-1865.
45. Matsumoto Ki, Takase K, Yamamoto Y, Doi Y, Taguchi S: **Chimeric enzyme composed of polyhydroxyalkanoate (PHA) synthases from *Ralstonia eutropha* and *Aeromonas caviae* enhances production of PHAs in recombinant *Escherichia coli*.** *Biomacromolecules* 2009, **10:**682-685.
46. Jahns AC, Rehm BH: **Tolerance of the Ralstonia eutropha class I polyhydroxyalkanoate synthase for translational fusions to its C terminus reveals a new mode of functional display.** *Appl Environ Microbiol* 2009, **75:**5461-5466.
47. Ushimaru K, Motoda Y, Numata K, Tsuge T: **Phasin proteins activate *Aeromonas caviae* polyhydroxyalkanoate (PHA) synthase but not *Ralstonia eutropha* PHA synthase.** *Applied and environmental microbiology* 2014, **80:**2867-2873.
48. Madden LA, Anderson AJ, Shah DT, Asrar J: **Chain termination in polyhydroxyalkanoate synthesis: involvement of exogenous hydroxy-compounds as chain transfer agents.** *International journal of biological macromolecules* 1999, **25:**43-53.
49. Nikel PI, De Almeida A, Melillo EC, Galvagno MA, Pettinari MJ: **New recombinant *Escherichia coli* strain tailored for the production of poly (3-hydroxybutyrate) from agroindustrial by-products.** *Applied and Environmental Microbiology* 2006, **72:**3949-3954.
50. Kurja J, Zirkzee HF, De Koning GM, Maxwell IA: **A new kinetic model for the accumulation of poly (3-hydroxybutyrate) in *Alcaligenes eutrophus*, 1. Granule growth.** *Macromolecular theory and simulations* 1995, **4:**839-855.
51. Koizumi F, Abe H, Doi Y: **Molecular weight of poly (3-hydroxybutyrate) during biological polymerization in *Alcaligenes eutrophus*.** *Journal of Macromolecular Science, Part A: Pure and Applied Chemistry* 1995, **32:**759-774.
52. Chanprateep S, Katakura Y, Visetkoop S, Shimizu H, Kulpreecha S, Shioya S: **Characterization of new isolated *Ralstonia eutropha* strain A-04 and kinetic study of biodegradable copolyester poly (3-hydroxybutyrate-co-4-hydroxybutyrate) production.** *Journal of industrial microbiology & biotechnology* 2008, **35:**1205-1215.
53. Sambrook J, Russell DW: **Molecular cloning: a laboratory manual. 2001.** Cold Spring Harbor Laboratory Press, Cold Spring Harbor, New York; 2001.
54. Braunegg G, Sonnleitner B, Lafferty R: **A rapid gas chromatographic method for the determination of poly-β-hydroxybutyric acid in microbial biomass.** *Applied Microbiology and Biotechnology* 1978, **6:**29-37.
55. Miller GL: **Use of dinitrosalicylic acid reagent for determination of reducing sugar.** *Analytical chemistry* 1959, **31:**426-428.
56. Yoshie N, Menju H, Sato H, Inoue Y: **Complex composition distribution of poly(3-hydroxybutyrate-co-3-hydroxyvalerate).** *Macromolecules* 1995, **28:**6516-6521.
57. Kang Z, Wang Q, Zhang H, Qi Q: **Construction of a stress-induced system in *Escherichia coli* for efficient polyhydroxyalkanoates production.** *Applied microbiology and biotechnology* 2008, **79:**203-208.
58. Wei X-X, Shi Z-Y, Yuan M-Q, Chen G-Q: **Effect of anaerobic promoters on the microaerobic production of polyhydroxybutyrate (PHB) in recombinant *Escherichia coli*.** *Applied microbiology and biotechnology* 2009, **82:**703.
59. Horng YT, Chang KC, Chien CC, Wei YH, Sun YM, Soo PC: **Enhanced polyhydroxybutyrate (PHB) production via the coexpressed *phaCAB* and *vgb* genes controlled by arabinose P_{BAD} promoter in *Escherichia coli*.** *Letters in applied microbiology* 2010, **50:**158-167.

Tables

Table 1 Bacterial strains and plasmids used in this study

Strains/plasmids	Relevant description	Reference/source
Strain		
Cupriavidus necator strain A-04	Wild Type	[33]
Escherichia coli JM109	F´ *traD36 proA+B+ lacI^q(lacZ)ΔM15/Δ(lac-proAB) glnV44 e14- gyrA96 recA1 relA1 endA1 thi hsdR17*	Promega Corporation, Madison, WI
Plasmid		
pUC19	Amp^r	Thermo Scientific, MA, USA
pColdI	Amp^r, lacI, cold-shock cspA promoter	Takara Bio Inc., Shiga, Japan
pColdIF	Amp^r, lacI, cold-shock cspA promoter and trigger factor	Takara Bio Inc., Shiga, Japan
pGEX-6P-1	Amp^r, lacI, tac promoter and glutathione S-transferase (GST)	Novagen, WI, USA
pBAD/Thio-TOPO	Amp^r, araBAD promoter and thioredoxin	Invitrogen, CA, USA
pUC19-nativeP-*phaCAB*$_{A-04}$	pUC19 derivative, carrying *phaCAB* with native promoter from *C. necator* strain A-04	This study
pColdI-*phaCAB*$_{A-04}$	pColdI derivative, carrying N-terminal 6His-fused *phaCAB* from *C. necator* strain A-04	This study
pColdTF-*phaCAB*$_{A-04}$	pColdTF derivative, carrying N-terminal 6His-fused *phaCAB* from *C. necator* strain A-04	This study
pGEX-6P-1- *phaCAB*$_{A-04}$	pGEX-6P-1 derivative, carrying N-terminal GST and 6His-fused *phaCAB* from *C. necator* strain A-04	This study
pBAD/Thio-TOPO-*phaCAB*$_{A-04}$	pBAD/Thio-TOPO® derivative, carrying C-terminal 6HIS- and N-terminal thioredoxin fused *phaCAB* from *C. necator* strain A-04	manuscript in preparation
Primer		
pCold-F	5'-ATGGATCCCTCGAGATGGCGACCGGCAAAG-3'	This study
pCold-R	5'-GTGAATTCAAGCTTTCAGCCCATATGCAGGCC-3'	This study
pGEX-F	5'-GGCCCCTGGGATCCCCGGAAATGGCGACCGGCAA-3'	This study
pGEX-R	5'- GCACTCGACTCGAGTCAGCCCATATGCAGG -3'	This study
nativeP-*phaCAB*$_{A-04}$-F	5'- TGGTCCCTGACTGGC-3'	This study
nativeP-*phaCAB*$_{A-04}$-R	5'- CGTCGACGACCTTGAAT-3'	This study

Table 2 Effect of IPTG concentration on CDM (g/L), PHB (g/L), % (w/w) PHB content and PHB productivity in a comparison between *E. coli* JM109 harboring pColdI-*phaCAB*$_{A-04}$ and *E. coli* JM109 harboring pColdTF-*phaCAB*$_{A-04}$

Plasmid	Inoculum % (v/v)	IPTG (mM)	CDM (g/L)	RCM (g/L)	PHB (g/L)	PHB content (% w/w)	Productivity g/(L×h)
pColdI-*phaCAB*$_{A-04}$							
short induction	5	0	2.8 ± 0.1	2.5 ± 0.1	0.3 ± 0.0	10.7 ± 1.1	0.01 ± 0.00
		0.01	2.8 ± 0.2	1.0 ± 0.2	1.8 ± 0.1	64.3 ± 3.1	0.07 ± 0.03
		0.05	2.6 ± 0.3	0.7 ± 0.2	1.9 ± 0.2	73.1 ± 3.5	0.08 ± 0.04
		0.1	2.6 ± 0.2	0.5 ± 0.1	2.1 ± 0.2	80.8 ± 0.7	0.08 ± 0.05
		0.5	4.5 ± 0.3	0.6 ± 0.1	3.9 ± 0.1	86.7 ± 2.6	0.16 ± 0.07
		1	2.6 ± 0.1	0.4 ± 0.0	2.2 ± 0.1	84.6 ± 0.6	0.09 ± 0.02
conventional induction	5	0.5	1.3 ± 0.1	0.7 ± 0.0	0.6 ± 0.1	46.6 ± 3.8	0.03 ± 0.01
preinduction	1	0.5	0.8 ± 0.0	0.7 ± 0.0	0.1 ± 0.0	8.35 ± 1.3	0.001 ± 0.00
	5	0.5	2.8 ± 0.6	0.9 ± 0.3	1.9 ± 0.6	66.6 ± 4.8	0.04 ± 0.01
	10	0.5	4.5 ± 1.1	1.0 ± 0.5	3.5 ± 1.1	78.7 ± 7.5	0.07 ± 0.02
pColdTF-*phaCAB*$_{A-04}$							
short induction	5	0	2.5 ± 0.1	2.3 ± 0.2	0.2 ± 0.0	8.0 ± 0.8	0.01 ± 0.00
		0.01	2.5 ± 0.2	1.1 ± 0.2	1.4 ± 0.1	56.0 ± 3.7	0.06 ± 0.02
		0.05	2.7 ± 0.2	0.9 ± 0.1	1.8 ± 0.1	66.7 ± 3.5	0.07 ± 0.03
		0.1	2.8 ± 0.5	0.8 ± 0.2	2.0 ± 0.3	71.4 ± 2.2	0.08 ± 0.08
		0.5	3.5 ± 0.5	0.7 ± 0.2	2.8 ± 0.3	80.0 ± 2.9	0.12 ± 0.07
		1	2.9 ± 0.2	0.7 ± 0.0	2.2 ± 0.2	75.9 ± 0.8	0.09 ± 0.04

Short induction was performed with 0.5 mM IPTG at 15°C for 30 min, and cultivation was performed at 37°C for 24 h.

Conventional induction was performed with 0.5 mM IPTG at 15°C, and cultivation was performed at 15°C for 24 h.

Preinduction was performed with 0.5 mM IPTG at 15°C for 24 h, and cultivation was performed at 37°C for 24 h.

Table 3 Comparison of the kinetics of cell growth, (g PHB/g-glucose), and PHB production g/(L×h) by *C. necator* strain A-04, *E. coli* JM109 (pColdI-*phaCAB*$_{A-04}$), *E. coli* JM109 (pColdTF-*phaCAB*$_{A-04}$), *E. coli* JM109 (pGEX-6P-1- *phaCAB*$_{A-04}$), *E. coli* JM109 (pBAD/Thio-TOPO- *phaCAB*$_{A-04}$), and *E. coli* JM109 (pUC19-nativeP-*phaCAB*$_{A-04}$) in shake flask cultivation.

Kinetic parameters	pColdI-*phaCAB*$_{A-04}$	pColdI-*phaCAB*$_{A-04}$	pColdTF-*phaCAB*$_{A-04}$	pColdTF-*phaCAB*$_{A-04}$	pGEX-6P-1-*phaCAB*$_{A-04}$	pBAD/Thio-TOPO-*phaCAB*$_{A-04}$	pUC19-nativeP-*phaCAB*$_{A-04}$
Temperature (°C)	15*	37	15*	37	37	37	37
Maximum PHB concentration (g/L)	1.4 ± 0.2	2.6 ± 0.2	1.3 ± 0.1	2.5 ± 0.1	0.9 ± 0.2	0.8 ± 0.2	0.7 ± 0.1
Maximum cell dry weight (g/L)	1.7 ± 0.1	2.9 ± 0.2	1.7 ± 0.2	2.8 ± 0.1	1.3 ± 0.1	1.2 ± 0.2	1.1 ± 0.2
Maximum PHB content (%w/w)	85.2 ± 2.5	89.9 ± 0.8	84.8 ± 3.3	90.6 ± 4.3	69.2 ± 2.6	66.7 ± 1.8	63.6 ± 2.2
Specific growth rate (1/h)	0.001	0.001	0.001	0.001	0.003	0.003	0.004
Specific consumption rate (g glucose/g CDM/h)	1.03	0.75	0.73	1.13	0.56	0.31	0.5
Specific production rate (g PHB/g CDM/h)	0.09	0.19	0.07	0.29	0.05	0.03	0.05
(g CDM/g glucose)	0.001	0.002	0.01	0.001	0.008	0.026	0.01
(g PHB/g glucose)	0.07	0.18	0.08	0.18	0.08	0.10	0.06
Productivity (g/(L×h)	0.03	0.09	0.03	0.10	0.02	0.03	0.02
Time (h)	48	30	48	24	48	30	30

The induction was performed with 0.5 mM IPTG at 15°C for 30 min, and then, cultivation was performed at 37°C for 48 h.

*The induction was performed with 0.5 mM IPTG at 15°C, and cultivation was performed at 15°C for 48 h.

Table 4 Quantification of purified soluble phaC$_{A-04}$ produced by *E. coli* JM109 (pColdI-*phaCAB*$_{A-04}$) and *E. coli* JM109 (pColdTF-*phaCAB*$_{A-04}$) under short induction method compared with the conventional method in shake flask cultivation.

Strains	Induction method	Initial protein loading (μg)	Total protein obtained after purification (μg)	% recovery	Total soluble his-tagged $phaC_{A-04}$	Soluble his-tagged $phaC_{A-04}$ (%)
pColdI-*phaCAB*$_{A-04}$	short induction	2,000	1,855 ± 75	93 ± 3.8	66 ± 2.8	3.6 ± 1.4
pColdTF-*phaCAB*$_{A-04}$	short induction	2,000	1,933 ± 28	97 ± 1.4	287 ± 37	14.8 ± 1.7
pColdI-*phaCAB*$_{A-04}$	conventional induction	2,000	1,795 ± 53	90 ± 2.7	274 ± 36	15.3 ± 2.3
pColdTF-*phaCAB*$_{A-04}$	conventional induction	2,000	1,880 ± 106	94 ± 5.3	890 ± 95	47.4 ± 2.4

The short induction was performed at 15°C for 30 min with 0.5 mM IPTG, and then cultivation was performed at 37°C for 48 h.

The conventional induction was performed at 15°C with 0.5 mM IPTG at 15°C, and cultivation was performed at 15°C for 48 h.

The experiments were performed as $n = 3$ technical replicates, and the results are expressed as the mean values ± standard errors (SEs).

Table 5 Comparison of kinetic parameters, molecular weight, and thermal and mechanical properties of PHB produced by *C. necator* strain A-04, *E. coli* JM109 (pColdI-*phaCAB*$_{A-04}$), *E. coli* JM109 (pColdTF-*phaCAB*$_{A-04}$) and *E. coli* JM109 (pUC19-nativeP-*phaCAB*$_{A-04}$)

Kinetic parameters and polymer properties of PHB	*C. necator* A-04		pColdTF-*phaCAB*$_{A-04}$	pColdI-*phaCAB*$_{A-04}$		pUC19-nativeP-*phaCAB*$_{A-04}$
	fructose*	raw sugar	glucose	glucose	crude glycerol	crude glycerol
Carbon source (g/L)	20	30	20	20	20	20
Maximum PHB concentration (g/L)	5.8 ± 0.5	4.7 ± 0.2	7.9 ± 0.7	5.8 ± 0.1	2.0 ± 0.1	2.1 ± 0.1
Maximum cell dry weight (g/L)	7.4 ± 1.5	7.3 ± 1.2	8.8 ± 0.5	7.2 ± 0.3	4.0 ± 0.2	3.93 ± 0.3
Maximum PHB content (%wt)	79.0 ± 1.9	68.9 ± 2.8	90.0 ± 2.3	78.0 ± 2.1	50.6 ± 3.0	53.4 ± 2.2
Specific growth rate (1/h)	0.003	0.001	0.07	0.06	0.08	0.11
Specific consumption rate (g carbon source/g CDM/h)	0.14	0.05	0.52	0.35	ND	ND
Specific production rate (g PHB/g CDM/h)	0.012	0.019	0.20	0.11	ND	ND
(g CDM/g-carbon source)	0.08	0.03	0.07	0.10	ND	ND
(g PHB/g carbon source)	0.29	0.35	0.38	0.32	ND	ND
Productivity (g/(L×h)	0.10	0.07	0.43	0.24	0.11	0.07
M_w ($\times 10^5$)	6.51	3.30	5.79	8.41	2.42	10.68
M_n ($\times 10^5$)	3.61	1.46	1.86	2.03	0.89	2.60
PDI	1.80	2.15	3.11	4.14	2.92	4.10
Young's modulus (MPa)	1497	1734	5465	2156	1980	2262
Tensile strength (MPa)	17.4	11.9	56.2	21.5	19.3	17.4
Elongation at break (%)	0.4	1.1	1.2	1.7	2.0	1.1
T_m (°C)	178	173	168	176	170	174
T_g (°C)	2.4	3.5	1.6	3.0	1.9	2.8
Time (h)	60	60	18	30	18	30

ND - not determined

* results from [35]

Table 6 Comparison of PHB production by recombinant *E. coli* reported previously

Strain	Gene source	Plasmid	Promoter	Time (h)	Operation	Carbon	CDM (g/L)	PHB (g/L)	% PHB (w/w)		Reference
JM109	*C. necator* strain A-04	pColdI-*phaCAB*$_{A-04}$	P_{cspA}	36	Batch	2% (w/v) glucose	7.2±0.3	5.8±0.1	78.0±2.1	0.32	This study
JM109	*C. necator* strain A-04	pColdTF-*phaCAB*$_{A-04}$	P_{cspA}	18	Batch	2% (w/v) glucose	8.6±0.3	7.0±0.3	82.9±0.3	0.29	This study
JM109	*C. necator* strain A-04	pColdTF-*phaCAB*$_{A-04}$	P_{cspA}	30	Batch	2% (w/v) glucose	8.8±0.5	7.9±0.7	90.0±2.3	0.38	This study
DH5α	*C. necator* H16	pQKZ103	P_{rpoS}	48	Flask	1.5% (w/v) glucose	4.1	3.52	85.8	-	[57]
JW2294	*C. necator* H16	pWYC09	P_{adhE}	24	Batch w/o air supply	3% (w/v) glucose	7.8±1.8	5.0±1.5	64.3±7.4	-	[58]
BW25113	*C. necator* H16	pWYC09	P_{adhE}	24	Batch w/o air supply	3% (w/v) glucose	6.7±1.6	3.0±1.3	45.5±3.9	-	[58]
JM109	*C. necator* H16	pBHR68	nativeP	48	Flask	1% (w/v) glucose	1.7±0.1	0.5	29.7±3.4	-	[58]
JM109	*C. necator* H16	pWYC09	P_{adhE}	48	Flask	1% (w/v) glucose	1.7±0.2	0.8	48.2±4.5	-	[58]
XL1-Blue	*C. necator* H16	pBAD24+ vgb gene	P_{BAD}	48	Flask	1% (w/v) glycerol	4.1±0.1	2.0±0.1	49.2±0.19	-	[59]
JM109	*C. necator* strain A-04	pBAD/Thio-TOPO	P_{BAD}	30	Flask	2% (w/v) glucose	1.2±0.2	0.8±0.2	67.2±1.8	0.10	This study
DH5α	*C. necator* H16	pGEM-GST*phaCAB*$_{Re}$	nativeP	72	Flask	2% (w/v) glucose	2.8±0.2	0.9±0.2	31±1	-	[32]
JM109	*C. necator* strain A-04	pGEX-6P-1	P_{tac}	48	Flask	2% (w/v) glucose	1.3 ± 0.1	0.9±0.2	74.6±2.6	-	This study
XL-1 blue	*C. necator* H16	pJRDTrc*phaCAB*$_{Re}$	P_{trc}	48	Fed-batch	>2% (w/v) glucose	178	128	72	-	[31]

Figures

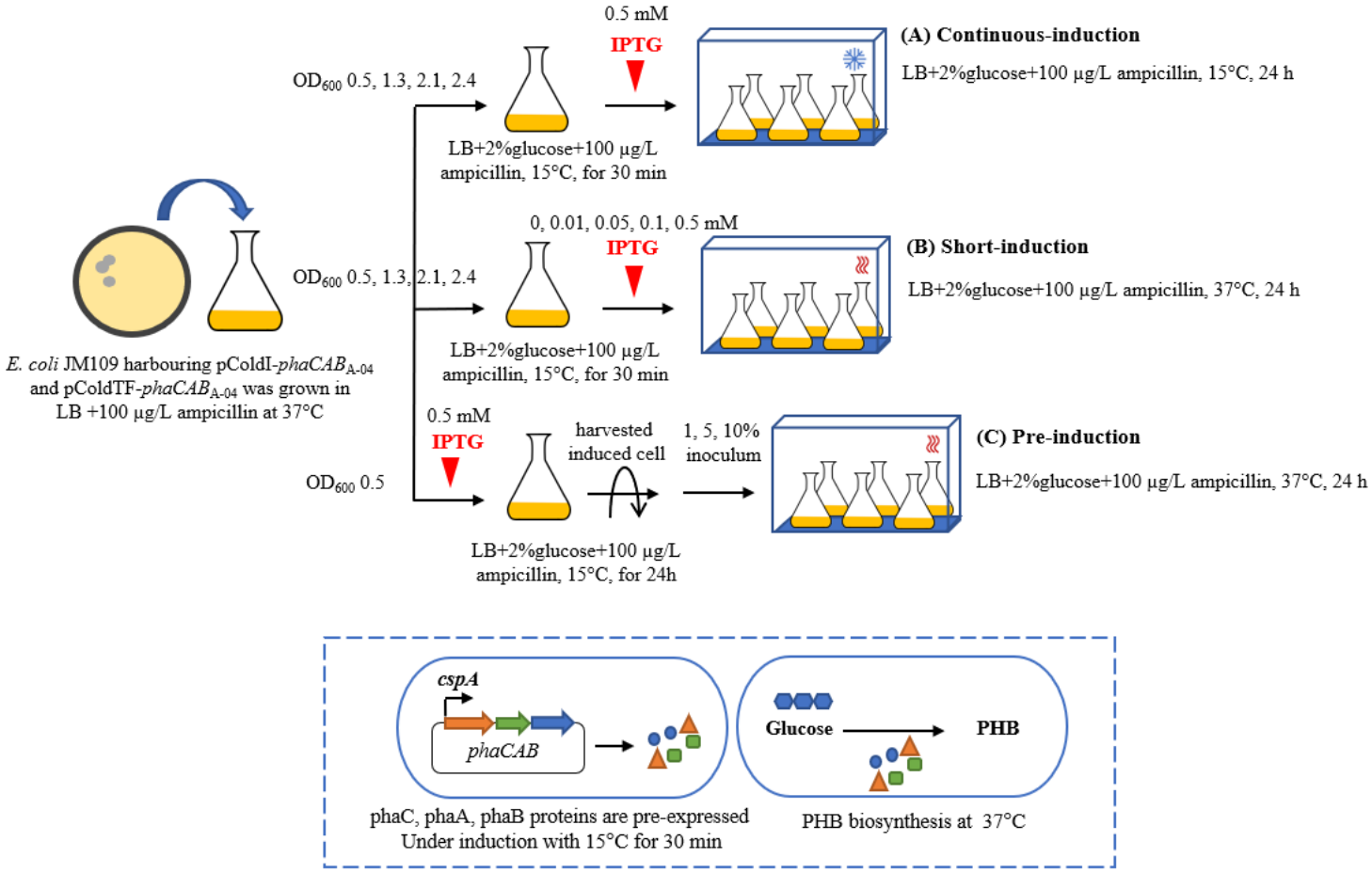

Figure 1

Schematic of three different induction methods for heterologous expression of the phaCABA-04 biosynthesis operon in E. coli JM109 (pColdI-phaCABA-04) and E. coli JM109 (pColdTF-phaCABA-04). (A) Conventional induction method: the culture was incubated at 37°C and 200 rpm until the OD600 reached 0.5, 1.3, 2.1 and 2.4. Then, the cultivation temperature was decreased from 37°C to 15°C for 30 min, and the expression of the phaCABA-04 operon was induced by the addition of 0.5 mM IPTG. The cultivation temperature was further maintained at 15°C for 24 h. (B) Short-induction method: the culture was incubated at 37°C and 200 rpm until the OD600 reached 0.5, 1.3, 2.1 and 2.4. Then, the temperatures were varied at 15, 25, 30 and 37°C for 30 min. Next, the expression of the phaCABA-04 operon was induced by adding various concentrations (0.01, 0.05, 0.1, 0.5 and 1.0 mM) of IPTG, and the cultivation temperature was maintained at 37°C for 24 h. (C) Preinduction method: the culture was incubated at 37°C and 200 rpm until the OD600 reached 0.5. Next, 0.5 mM IPTG was added into the culture when the temperature was decreased from 37°C to 15°C for 24 h. Then, the induced cells were harvested by centrifugation, the medium was discarded, and the cells were resuspended in an equal volume of fresh LB medium. Finally, the induced cells at 1, 5 or 10% (v/v) were transferred into fresh LB medium supplemented with 100 □g/L ampicillin and 20 g/L glucose and incubated at 37°C and 200 rpm for 24 h.

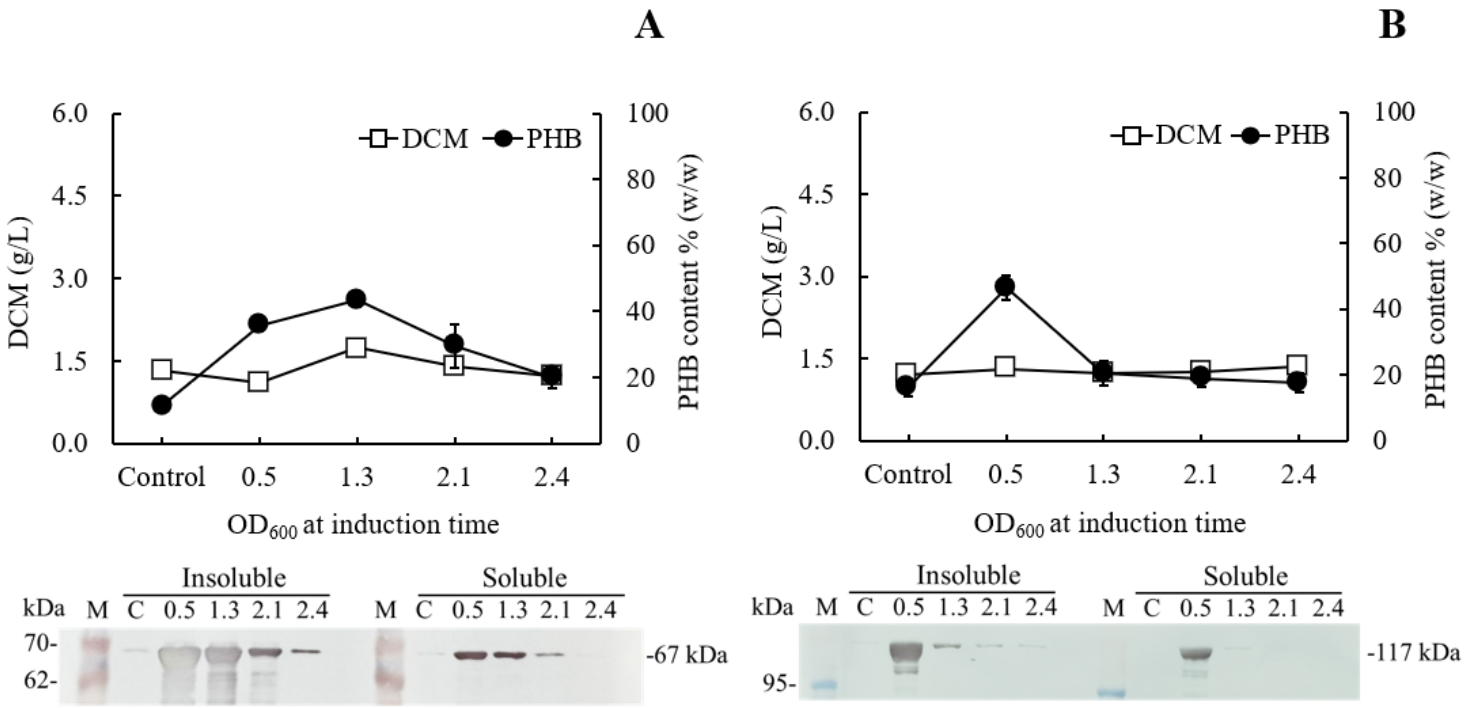

Figure 2

Effect of the growth phase suitable for cold-shock induction on CDM and PHB content (% w/w) under the conventional induction method. The different growth phases were investigated by varying OD600 based on cultivation time (0.5 (2 h, early exponential phase), 1.3 (4 h, middle exponential phase), 2.1 (6 h, late exponential phase) and 2.4 (10 h, stationary phase)) for (A) E. coli JM109 (pColdI-phaCABA-04) and (B) E. coli JM109 (pColdTF-phaCABA-04). A control experiment was performed with 0.0 mM IPTG induction. All the data are representative of the results of three independent experiments and are expressed as the mean values ± standard deviations (SDs). The PhaCA-04 protein was detected by western blot analysis using anti-His tag antibody as the primary antibody. The band appearing in the western blot at the position corresponding to that of the His-tagged phaCA-04 protein was 67 kDa in size for pColdI-phaCABA-04, and the fusion protein of His-tagged phaCA-04 and TF was 115 kDa in size. All the data are representative of the results of three independent experiments and are expressed as the mean values ± standard deviations (SDs).

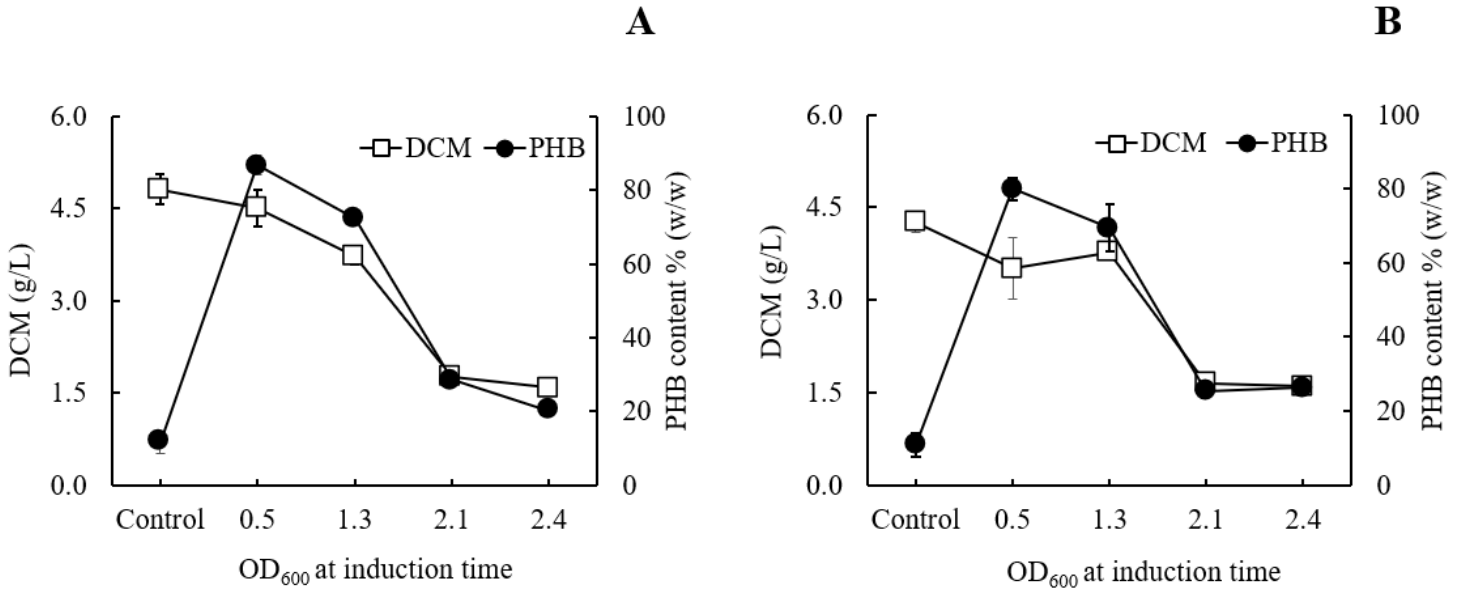

Figure 3

Effect of the growth phase suitable for cold-shock induction on CDM and PHB content (% w/w) under the short-induction method. The different growth phases were investigated by varying OD600 based on cultivation time (0.5 (2 h, early exponential phase), 1.3 (4 h, middle exponential phase), 2.1 (6 h, late exponential phase) and 2.4 (10 h, stationary phase)) for (A) E. coli JM109 (pColdI-phaCABA-04) and (B) E. coli JM109 (pColdTF-phaCABA-04). A control experiment was performed with 0.0 mM IPTG induction. All the data are representative of the results of three independent experiments and are expressed as the mean values ± standard deviations (SDs).

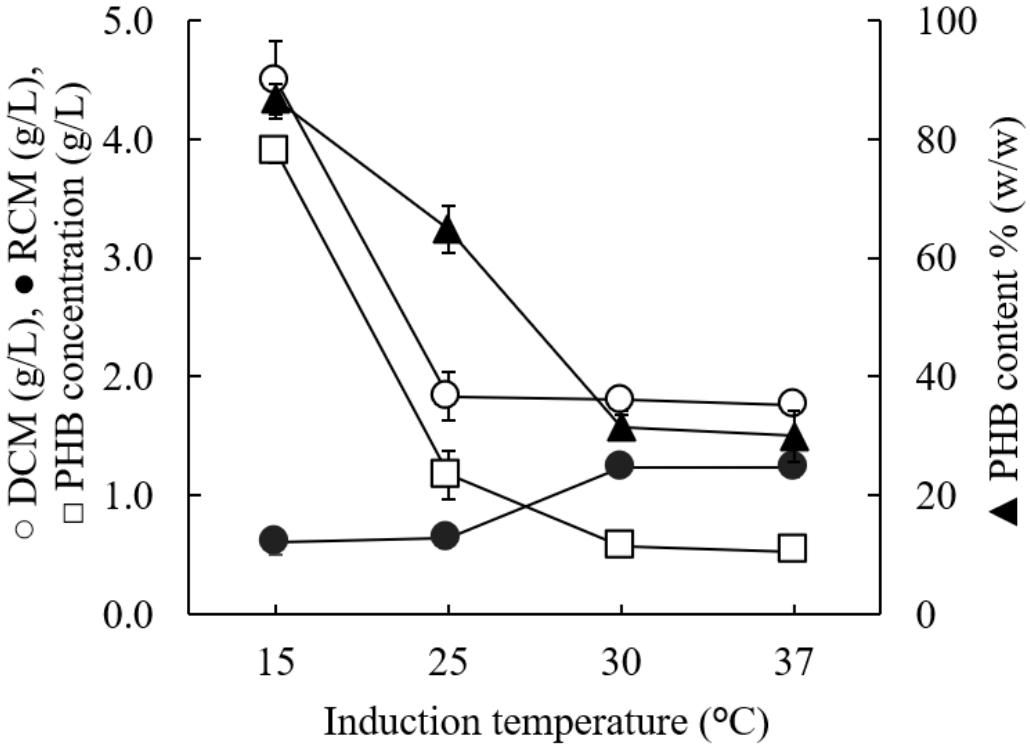

Figure 4

Effect of different short-induction temperatures (15, 25, 30 and 37°C) on the CDM (g/L), RCM (g/L), PHB (g/L) and PHB content (% w/w) of E. coli JM109 (pColdI-phaCABA-04). All the data are representative of the results of three independent experiments and are expressed as the mean values ± standard deviations (SDs).

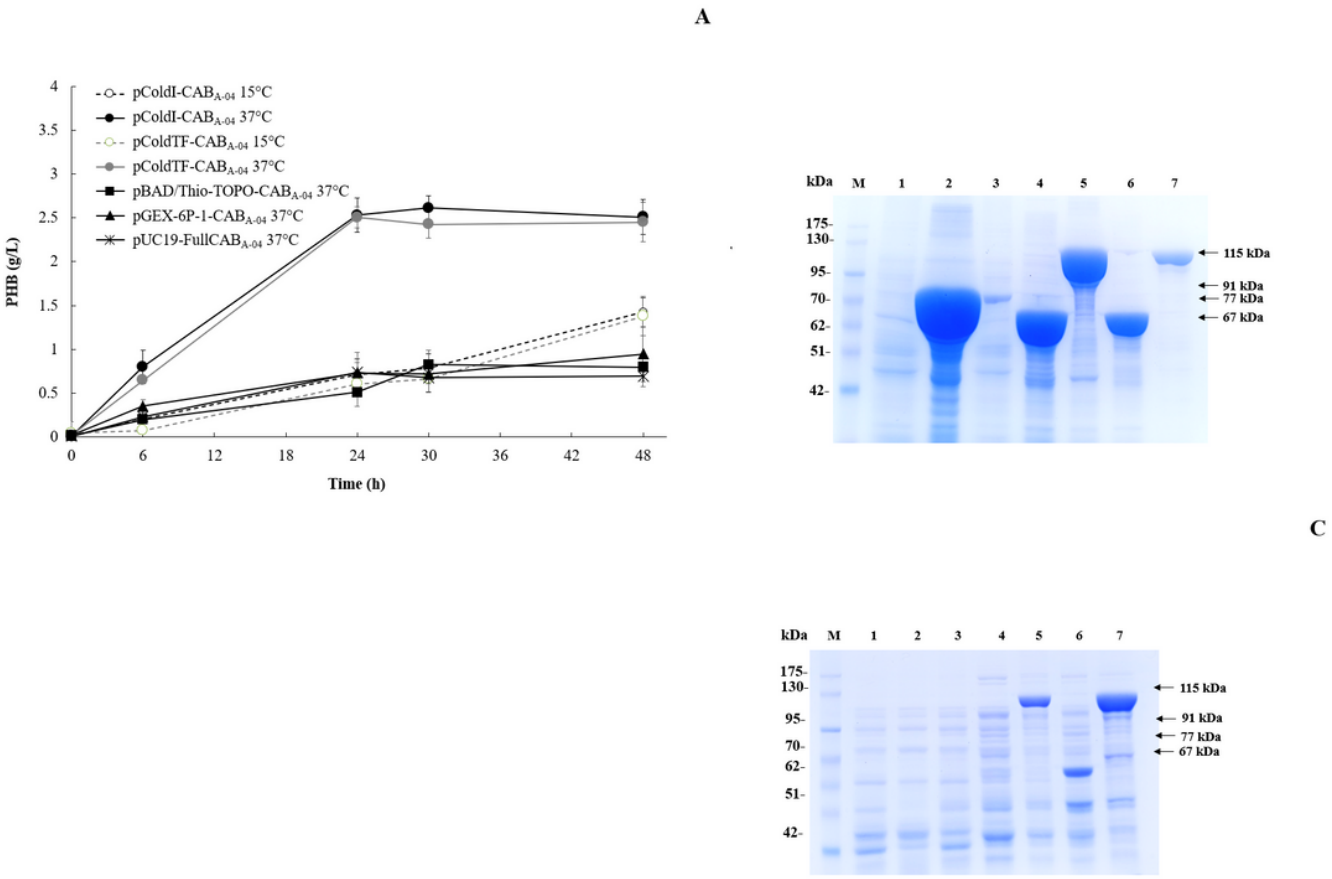

Figure 5

PHB production by pColdI-phaCABA-04, pColdTF-phaCABA-04, pGEX-6P-1-phaCABA-04, pBAD/Thio-TOPO-phaCABA-04 and pUC19-nativeP-phaCABA-04 in shake flask cultivation. (A) Time courses of PHB production (g/L). (B) The insoluble PhaCA-04 protein was confirmed by SDS-PAGE analysis (20 µg of total protein was loaded in each lane). (C) The soluble PhaCA-04 protein was confirmed by SDS-PAGE analysis (20 µg of total protein was loaded in each lane). Lane M, Protein molecular weight marker; lane 1, E. coli JM109 (pUC19-nativeP-phaCABA-04) under short induction temperature profile, but without addition of IPTG; lane 2, E. coli JM109 pBAD/Thio-TOPO- phaCABA-04 under short induction method; lane 3, E. coli JM109 (pGEX-6P-1- phaCABA-04) under short induction method; lane 4, E. coli JM109 (pColdI-phaCABA-04) under short induction method; lane 5, E. coli JM109 (pColdTF-phaCABA-04) under short induction method; lane 6, E. coli JM109 (pColdI-phaCABA-04) under conventional induction method; lane 7, E. coli JM109 (pColdTF-phaCABA-04) under conventional induction method. The band appearing in the SDS-PAGE at the position corresponding to that of the phaCA-04 protein was 64 kDa in size for pUC19-nativeP-phaCABA-04, His-tagged phaCA-04 fusion protein was 67 kDa in size for pColdI-phaCABA-04, thioredoxin-tagged phaCA-04 fusion protein was 77 kDa in size for pBAD/Thio-TOPO-phaCABA-04, GST-tagged phaCA-04 fusion protein was 91 kDa in size for pGEX-6P-1-phaCABA-04, and the fusion protein of His-tagged phaCA-04 and TF was 115 kDa in size for pColdTF-phaCABA-04.

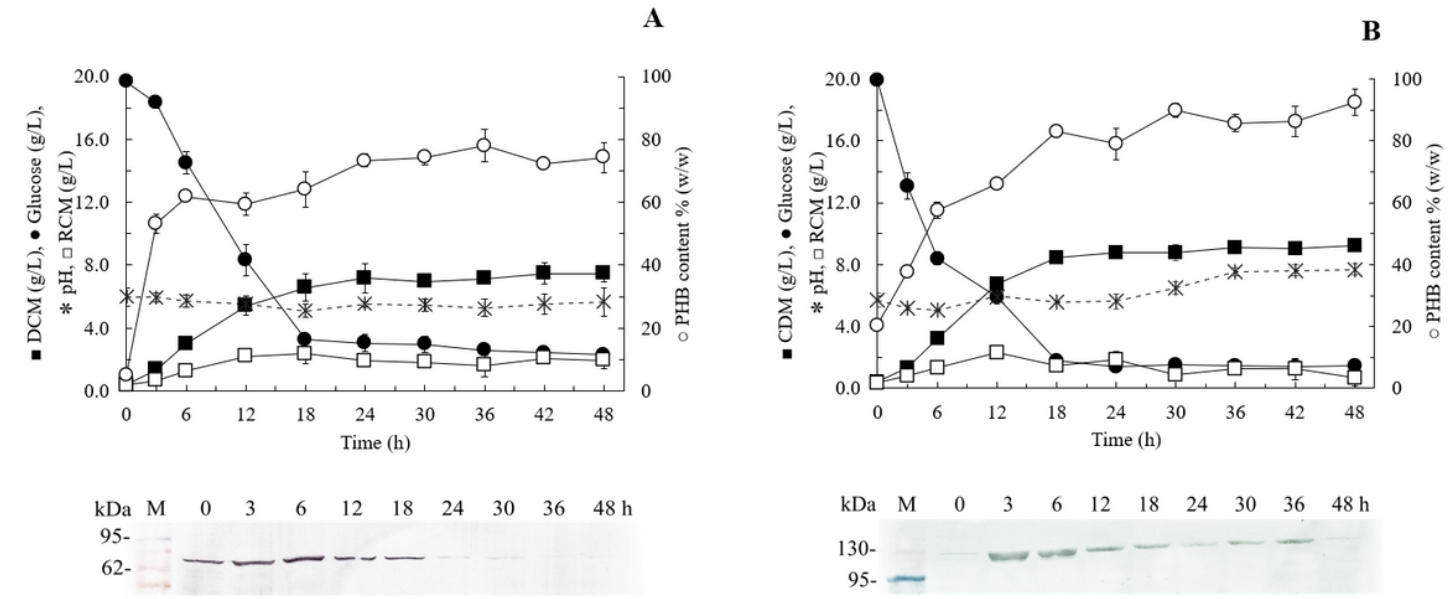

Figure 6

Time courses of CDM (g/L), RCM (g/L), PHB (g/L), PHB content (% w/w), and glucose (g/L) and pH during batch cultivation in a 5-L fermenter under the short-induction method in a comparison between (A) E. coli JM109 (pColdI-phaCABA-04) and (B) E. coli JM109 (pColdTF-phaCABA-04). The band appearing in the western blot at the position corresponding to that of the His-tagged phaCA-04 protein was 67 kDa in size for pColdI-phaCABA-04, and the fusion protein of His-tagged phaCA-04 and TF was 115 kDa in size. All the data are representative of the results of three independent experiments and are expressed as the mean values ± standard deviations (SDs).

Figure 7

Morphology of PHB films produced by (A) C. necator strain A-04, (B) E. coli JM109 (pColdI-phaCABA-04) and (C) E. coli JM109 (pColdTF-phaCABA-04).

Supplementary Files

This is a list of supplementary files associated with this preprint. Click to download.

- BBIOD2000176R1NapathornSupplementaryfinal.docx
- FigureS1BBIONapathorn2020FINAL.pptx